

**SYNTHESIS AND MESOMORPHIC PROPERTIES OF SYMMETRIC AND
NON-SYMMETRIC MULTI-FUNCTIONALIZED OLIGOMERS**

by

HNG TIANG CHUAN

**Thesis submitted in fulfillment of the requirements
for the degree of
Doctor of Philosophy**

February 2009

ACKNOWLEDGEMENT

I wish to take this opportunity to thank my main supervisor, Professor Yeap Guan Yeow for his teaching and attention to my research throughout the period of my candidature. Also, I would like to express my appreciation to my co-supervisor, Professor Wan Ahmad Kamil Mahmood for giving me advice and assistance generously. I wish to thank the Dean and the staff of School of Chemical Sciences for providing me with the research facilities. My gratitude also goes to the Dean of Institute of Postgraduate Studies for giving me a chance to enroll as a PhD student at Universiti Sains Malaysia.

I would like to express my sincere appreciation to Professor Masato M. Ito of Soka University, Japan, Associate Professor Daisuke Takeuchi from Tokyo Institute of Technology, Japan and Professor Ewa Gorecka from Warsaw University, Poland for the assistance in several analyses on my liquid crystal samples. I wish to thank Professor Corrie T. Imrie of University of Aberdeen, Scotland, who is also my field supervisor, for sharing his expertise in liquid crystal research with me. I am also grateful to my laboratory mates for sharing their knowledge with me and providing me with great assistance in many aspects at the workplace.

To my family members and friends, I wish to convey my best regards and gratitude for their support all this while.

TABLE OF CONTENTS

ACKNOWLEDGEMENT	ii
TABLE OF CONTENTS	iii
LIST OF TABLES	ix
LIST OF FIGURES	xvi
ABSTRAK	xxxii
ABSTRACT	xxxiv
1.0 INTRODUCTION	
1.1 Liquid crystals: History	1
1.2 Liquid crystals: Concept	1
1.3 Mesophases	2
1.3.1 Nematic phase	2
1.3.1.1 Chiral nematic phase	3
1.3.2 Smectic phase	4
1.3.2.1 Non-chiral smectic phase	4
1.3.2.2 Chiral smectic phase	8
1.3.2.3 Unidentified smectic phase	9
1.3.3 Blue phase	9
1.4 Mesogen	10
1.4.1 Calamitic mesogens	10
1.4.2 Discotic mesogens	11
1.4.3 Banana-shaped mesogens	12
1.4.4 Laterally branched mesogens	12
1.4.5 Oligomeric mesogens	13

1.5	Structure-property relationship of liquid crystals	15
1.5.1	Structure-property relationship of liquid crystal oligomers	16
1.5.1.1	The influence of spacer length and parity on the liquid crystalline properties of oligomers	16
1.5.1.2	The influence of unlike cores and non-symmetric structures on the liquid crystalline properties of oligomers	17
1.5.2	Chirality effect on liquid crystalline properties	17
1.6	Application of liquid crystals	18
1.7	Objectives of the research	19
2.0	EXPERIMENTAL	
2.1	Chemicals	21
2.2	Equipment	22
2.3	Synthesis and characterization	23
2.3.1	First series α -(4-Benzylidene-substituted-aniline-4'-oxy)- ω -[2-methylbutyl-4'-(4''-phenyl)benzoateoxy]alkanes, 4a-4j	24
2.3.1.1	Synthesis of (<i>RS</i>)-2-methylbutyl-4'-(4''-hydroxy-phenyl)benzoate, 1	24
2.3.1.2	Synthesis of 4-hydroxy-4'-benzylidene-substituted-anilines, 2a-2e	24
2.3.1.3	Synthesis of 4-(<i>n</i> -bromoalkoxy)-4'-benzylidene-substituted-anilines, 3a-3j	25
2.3.1.4	Synthesis of α -(4-benzylideneaniline-4'-oxy)- ω -[2-methylbutyl-4'-(4''-phenyl)benzoateoxy]alkanes, 4a-4j	27
2.3.2	Second series α -(4-Benzylidenechloroaniline-4'-oxy)- ω -[4-(thiophene-2-carboxyl)-benzylideneaniline-4'-oxy]alkanes, 9a-9h	28
2.3.2.1	Synthesis of 4-formylphenyl thiophene-2-carboxylate, 5	29
2.3.2.2	Synthesis of 4-(thiophene-2-carboxyl)benzylidene-4'-hydroxyaniline, 6	30

2.3.2.3	Synthesis of 4-hydroxy-4'-benzylidenechloroaniline, 7 and 4-(<i>n</i> -bromoalkyloxy)-4'-benzylidenechloroanilines, 8a-8h	30
2.3.2.4	Synthesis of α -(4-benzylidenechloroaniline-4'-oxy)- ω -[4-(thiophene-2-carboxyl)benzylideneaniline-4'-oxy]alkanes 9a-9h	31
2.3.3	Third, fourth and fifth series 4,4'-Bis{ ω -[2-methylbutyl-4'-(4''-phenyl)benzoateoxy]alkyloxybenzylidene}-1,4-diaminobenzenes, 13a-13h , 4,4'-bis{ ω -[2-methylbutyl-4'-(4''-phenyl)benzoateoxy]-3-methoxy-4-alkyloxybenzylidene}-1,4-diaminobenzenes, 16a-16h and 4,4'-bis{ ω -[2-methylbutyl-4'-(4''-phenyl)benzoateoxy]-3-bromo-4-alkyloxybenzylidene}-1,4-diaminobenzenes, 19a-19h	32
2.3.3.1	Synthesis of (<i>S</i>)-(-)-2-methylbutyl-4'-(4''-hydroxyphenyl)-benzoate, 10	32
2.3.3.2	Synthesis of 4,4'-bis(4-hydroxybenzylidene)-1,4-diaminobenzene, 11 , 4,4'-bis(3-methoxy-4-hydroxybenzylidene)-1,4-diaminobenzene, 14 and 4,4'-bis(3-bromo-4-hydroxybenzylidene)-1,4-diaminobenzene, 17	34
2.3.3.3	Synthesis of 4,4'-bis[4-(<i>n</i> -bromoalkyloxy)benzylidene]-1,4-diaminobenzenes, 12a-12h , 4,4'-bis[3-methoxy-4-(<i>n</i> -bromoalkyloxy)benzylidene]-1,4-diaminobenzenes, 15a-15h and 4,4'-bis[3-bromo-4-(<i>n</i> -bromoalkyloxy)benzylidene]-1,4-diaminobenzenes, 18a-18h	34
2.3.3.4	Synthesis of 4,4'-bis{ ω -[2-methylbutyl-4'-(4''-phenyl)benzoateoxy]alkyloxybenzylidene}-1,4-diaminobenzenes, 13a-13h , 4,4'-bis{ ω -[2-methylbutyl-4'-(4''-phenyl)benzoateoxy]-3-methoxy-4-alkyloxybenzylidene}-1,4-diaminobenzenes, 16a-16h and 4,4'-bis{ ω -[2-methylbutyl-4'-(4''-phenyl)benzoateoxy]-3-bromo-4-alkyloxybenzylidene}-1,4-diaminobenzenes, 19a-19h	35
2.3.4	Sixth series 4-Ethyl- and 4-fluoroanilinebenzylidene-2',4'-oxybis(4''-halogenoanilinebenzylidene-4'''-oxy)alkanes, 25a-25d and 26a-26d	38
2.3.4.1	Synthesis of 4-hydroxy-4'-benzylidene-substituted-anilines, 22a and 22b	39
2.3.4.2	Synthesis of 4-(<i>n</i> -bromoalkyloxy)-4'-benzylidene-substituted-anilines, 23a-23d	39
2.3.4.3	Synthesis of benzyl-2,4-oxybis(4'-halogenoanilinebenzylidene-4'''-oxy)alkane aldehydes, 24a-24d	39

2.3.4.4	Synthesis of 4-ethyl- and 4-fluoroanilinebenzylidene-2',4'-oxy-bis(4''-halogenoanilinebenzylidene-4'''-oxy)alkanes, 25a-25d and 26a-26d	40
3.0	RESULTS AND DISCUSSION FOR α-(4-BENZYLIDENE-SUBSTITUTED-ANILINE-4'-OXY)-ω-[2-METHYLBUTYL-4'-(4''-PHENYL)BENZOATEOXY]ALKANES	
3.1	Physical characterization	42
3.1.1	(<i>RS</i>)-2-methylbutyl-4'-(4''-hydroxyphenyl)benzoate, 1	42
3.1.2	4-Hydroxy-4'-benzylidene-substituted-anilines, 2a-2e	50
3.1.3	4-(<i>n</i> -Bromoalkyloxy)-4'-benzylidene-substituted-anilines, 3a-3j	60
3.1.4	α -(4-Benzylidene-substituted-aniline-4'-oxy)- ω -[2-methylbutyl-4'-(4''-phenyl)benzoateoxy]alkanes, 4a-4j	72
3.2	Mesomorphic (liquid crystalline) properties	108
4.0	RESULTS AND DISCUSSION FOR α-(4-BENZYLIDENECHLORO-ANILINE-4'-OXY)-ω-[4-(THIOPHENE-2-CARBOXYL)-BENZYLIDENEANILINE-4'-OXY]ALKANES	
4.1	Physical characterization	118
4.1.1	4-Formylphenyl thiophene-2-carboxylate, 5	118
4.1.2	4-(Thiophene-2-carboxyl)benzylidene-4'-hydroxyaniline, 6	124
4.1.3	4-Hydroxy-4'-benzylidenechloroaniline, 7 and 4-(<i>n</i> -bromoalkyloxy)-4'-benzylidenechloroanilines, 8a-8h	130
4.1.4	α -(4-Benzylidenechloroaniline-4'-oxy)- ω -[4-(thiophene-2-carboxyl)-benzylideneaniline-4'-oxy]alkanes, 9a-9h	136
4.2	Mesomorphic (liquid crystalline) properties	157
5.0	RESULTS AND DISCUSSION FOR 4,4'-BIS{ω-[2-METHYLBUTYL-4'-(4''-PHENYL)BENZOATEOXY]ALKYLOXYBENZYLIDENE}-1,4-DIAMINOBENZENES	
5.1	Physical characterization	164
5.1.1	(<i>S</i>)-(-)-2-Methylbutyl-4'-(4''-hydroxyphenyl)benzoate, 10	164

5.1.2	4,4'-Bis(4-hydroxybenzylidene)-1,4-diaminobenzene, 11	169
5.1.3	4,4'-Bis[4-(<i>n</i> -bromoalkyloxy)benzylidene]-1,4-diaminobenzenes, 12a-12h	172
5.1.4	4,4'-Bis{ ω -[2-methylbutyl-4'-(4''-phenyl)benzoateoxy]alkyloxybenzylidene}-1,4-diaminobenzenes, 13a-13h	180
5.2	Mesomorphic (liquid crystalline) properties	212
6.0	RESULTS AND DISCUSSION FOR 4,4'-BIS{ω-[2-METHYLBUTYL-4'-(4''-PHENYL)BENZOATEOXY]-3-METHOXY-4-ALKYLOXY-BENZYLIDENE}-1,4-DIAMINO BENZENES	
6.1	Physical characterization	226
6.1.1	4,4'-Bis(3-methoxy-4-hydroxybenzylidene)-1,4-diaminobenzene, 14	226
6.1.2	4,4'-Bis[3-methoxy-4-(<i>n</i> -bromoalkyloxy)benzylidene]-1,4-diaminobenzenes, 15a-15h	230
6.1.3	4,4'-Bis{ ω -[2-methylbutyl-4'-(4''-phenyl)benzoateoxy]-3-methoxy-4-alkyloxybenzylidene}-1,4-diaminobenzenes, 16a-16h	238
6.2	Mesomorphic (liquid crystalline) properties	270
7.0	RESULTS AND DISCUSSION FOR 4,4'-BIS{ω-[2-METHYLBUTYL-4'-(4''-PHENYL)BENZOATEOXY]3-BROMO-4-ALKYLOXY-BENZYLIDENE}-1,4-DIAMINO BENZENES	
7.1	Physical characterization	274
7.1.1	4,4'-Bis(3-bromo-4-hydroxybenzylidene)-1,4-diaminobenzene, 17	274
7.1.2	4,4'-Bis[3-bromo-4-(<i>n</i> -bromoalkyloxy)benzylidene]-1,4-diaminobenzenes, 18a-18h	277
7.1.3	4,4'-Bis{ ω -[2-methylbutyl-4'-(4''-phenyl)benzoateoxy]-3-bromo-4-alkyloxybenzylidene}-1,4-diaminobenzenes, 19a-19h	285
7.2	Mesomorphic (liquid crystalline) properties	317
8.0	RESULTS AND DISCUSSION FOR 4-ETHYL- AND 4-FLUORO-ANILINEBENZYLIDENE-2',4'-OXYBIS(4''-HALOGENOANILINE-BENZYLIDENE-4''-OXY)ALKANES	
8.1	Physical characterization	325

8.1.1	4-Hydroxy-4'-benzylidene-substituted-anilines, 22a and 22b	325
8.1.2	4-(<i>n</i> -Bromoalkyloxy)-4'-benzylidene-substituted-anilines, 23a-23d	328
8.1.3	Benzyl-2,4-oxybis(4'-halogenoanilinebenzylidene-4''-oxy)alkane aldehydes, 24a-24d	335
8.1.4	4-Ethyl- and 4-fluoroanilinebenzylidene-2',4'-oxybis(4''-halogeno-anilinebenzylidene-4'''-oxy)alkanes, 25a-25d and 26a-26d	342
8.2	Mesomorphic (liquid crystalline) properties	378
9.0	CONCLUSIONS	389
	REFERENCES	393
	APPENDICES	
	Appendix A: International publications	
	Appendix B: Papers presented in international or regional conference / seminar	

LIST OF TABLES

Table 2.1	List of chemicals used for the syntheses and respective assays	21
Table 2.2	General molecular formula and amounts of corresponding anilines for the syntheses of compounds 2a-2e	25
Table 2.3	Amounts of compounds 2a-2e and corresponding α,ω -dibromoalkanes for the syntheses of compounds 3a-3j	27
Table 2.4	Amounts of compounds 3a-3j for the syntheses of compounds 4a-4j	28
Table 2.5	Amounts of corresponding α,ω -dibromoalkanes for the syntheses of compounds 8a-8h	30
Table 2.6	Amounts of compounds 8a-8h for the syntheses of compounds 9a-9h	31
Table 2.7	Amounts of corresponding α,ω -dibromoalkanes for the syntheses of compounds 12a-12h , 15a-15h and 18a-18h	35
Table 2.8	Amounts of compounds 10 and 12a-12h for the syntheses of compounds 13a-13h	36
Table 2.9	Amounts of compounds 10 and 15a-15h for the syntheses of compounds 16a-16h	37
Table 2.10	Amounts of compounds 10 and 18a-18h for the syntheses of compounds 19a-19h	37
Table 2.11	Amounts of compounds 22a , 22b and corresponding α,ω -dibromoalkanes for the syntheses of compounds 23a-23d	39
Table 2.12	Amounts of compounds 23a-23d for the syntheses of compounds 24a-24d	40
Table 2.13	Amounts of compounds 24a-24d , the general molecular formula and amounts of corresponding anilines for the syntheses of compounds 25a-25d	41
Table 3.1	C and H microanalytical data of compound 1	44
Table 3.2	Selected FT-IR absorption frequency (ν / cm^{-1}) of compound 1	44
Table 3.3	List of ^1H -NMR chemical shifts (δ / ppm), multiplicity, number of protons and associated functional groups of compound 1	47
Table 3.4	C, H and N microanalytical data of compounds 2a-2e	52
Table 3.5	Selected FT-IR absorption frequency (ν / cm^{-1}) of compounds 2a-2e	53

Table 3.6	List of ^1H -NMR chemical shifts (δ / ppm), multiplicity, number of protons and associated functional groups of compounds 2a-2e	60
Table 3.7	Yields (%) of compounds 3a-3j	62
Table 3.8	C, H and N microanalytical data of compounds 3a-3j	62
Table 3.9	Selected FT-IR absorption frequency (ν / cm^{-1}) of compounds 3a-3j	66
Table 3.10	List of ^1H -NMR chemical shifts (δ / ppm), multiplicity, number of protons and associated functional groups of compounds 3a-3j	71
Table 3.11	Yields (%) of compounds 4a-4j	73
Table 3.12	C, H and N microanalytical data of compounds 4a-4j	73
Table 3.13	Selected FT-IR absorption frequency (ν / cm^{-1}) of compounds 4a-4j	75
Table 3.14	Chemical shifts (δ / ppm) for the selected protons of compound 4b	81
Table 3.15	Chemical shifts (δ / ppm) for the selected carbons and ^1H - ^{13}C HMQC and HMBC correlations of compound 4b	91
Table 3.16	Chemical shifts (δ / ppm) for the quaternary carbons of compound 4b	92
Table 3.17	Chemical shifts (δ / ppm) for the selected protons of compound 4d	96
Table 3.18	Chemical shifts (δ / ppm) for the selected carbons and ^1H - ^{13}C HMQC and HMBC correlations of compound 4d	104
Table 3.19	Chemical shifts (δ / ppm) for the quaternary carbons of compound 4d	105
Table 3.20	Chemical shifts (δ / ppm) for the selected protons of compounds 4a, 4c and 4e-4j	106
Table 3.21	Chemical shifts (δ / ppm) for the selected carbons of compounds 4a, 4c and 4e	107
Table 3.22	Chemical shifts (δ / ppm) for the selected carbons of compounds 4f-4j	108
Table 3.23	The phase transition temperatures ($^{\circ}\text{C}$), associated enthalpy changes (kJmol^{-1}) and nematic-isotropic entropy changes of compounds 4a-4j . Virtual transition temperatures obtained by extrapolation of phase diagrams are given in []. Only the highest melting points are listed. (\bullet = enantiotropic phase, \circ = monotropic phase, Cr = crystal, SmA_c = intercalated SmA, N = nematic, I = isotropic)	109
Table 4.1	C and H microanalytical data of compound 5	120

Table 4.2	Selected FT-IR absorption frequency (ν / cm^{-1}) of compound 5	121
Table 4.3	List of ^1H -NMR chemical shifts (δ / ppm), multiplicity, number of protons and associated functional groups of compound 5	121
Table 4.4	C, H and N microanalytical data of compound 6	125
Table 4.5	Selected FT-IR absorption frequency (ν / cm^{-1}) of compound 6	126
Table 4.6	List of ^1H -NMR chemical shifts (δ / ppm), multiplicity, number of protons and associated functional groups of compound 6	127
Table 4.7	Yields (%) of compounds 8a-8h	131
Table 4.8	C, H and N microanalytical data of compounds 8a-8h	131
Table 4.9	Selected FT-IR absorption frequency (ν / cm^{-1}) of compounds 8a-8h	133
Table 4.10	List of ^1H -NMR chemical shifts (δ / ppm), multiplicity, number of protons and associated functional groups of compounds 8a-8h	135
Table 4.11	Yields (%) of compounds 9a-9h	137
Table 4.12	C, H and N microanalytical data of compounds 9a-9h	137
Table 4.13	Selected FT-IR absorption frequency (ν / cm^{-1}) of compounds 9a-9h	138
Table 4.14	Chemical shifts (δ / ppm) for the selected protons of compound 9c	142
Table 4.15	Chemical shifts (δ / ppm) for the selected carbons and ^1H - ^{13}C HMQC and HMBC correlations of compound 9c	154
Table 4.16	Chemical shifts (δ / ppm) for the quaternary carbons of compound 9c	155
Table 4.17	Chemical shifts (δ / ppm) for the selected protons of compounds 9a, 9b and 9d-9h	155
Table 4.18	Chemical shifts (δ / ppm) for the selected carbons of compounds 9a, 9b, 9d and 9e	156
Table 4.19	Chemical shifts (δ / ppm) for the selected carbons of compounds 9f-9h	156
Table 4.20	The phase transition temperatures ($^{\circ}\text{C}$), associated enthalpy changes (kJmol^{-1}) and nematic-isotropic entropy changes of compounds 9a-9h (\bullet = enantiotropic phase, Cr = crystal, N = nematic, I = isotropic)	158
Table 5.1	C and H microanalytical data of compound 10	165
Table 5.2	Selected FT-IR absorption frequency (ν / cm^{-1}) of compound 10	166

Table 5.3	List of ^1H -NMR chemical shifts (δ / ppm), multiplicity, number of protons and associated functional groups of compound 10	166
Table 5.4	C, H and N microanalytical data of compound 11	170
Table 5.5	Selected FT-IR absorption frequency (ν / cm^{-1}) of compound 11	170
Table 5.6	Yields (%) of compounds 12a-12h	173
Table 5.7	C, H and N microanalytical data of compounds 12a-12h	173
Table 5.8	Selected FT-IR absorption frequency (ν / cm^{-1}) of compounds 12a-12h	174
Table 5.9	List of ^1H -NMR chemical shifts (δ / ppm), multiplicity, number of protons and associated functional groups of compounds 12a-12h	180
Table 5.10	Yields (%) of compounds 13a-13h	181
Table 5.11	C, H and N microanalytical data of compounds 13a-13h	182
Table 5.12	Selected FT-IR absorption frequency (ν / cm^{-1}) of compounds 13a-13h	185
Table 5.13	Chemical shifts (δ / ppm) for the selected protons of compound 13c	187
Table 5.14	Chemical shifts (δ / ppm) for the selected carbons and ^1H - ^{13}C HMQC and HMBC correlations of compound 13c	191
Table 5.15	Chemical shifts (δ / ppm) for the quaternary carbons of compound 13c	198
Table 5.16	Chemical shifts (δ / ppm) for the selected protons of compound 13f	202
Table 5.17	Chemical shifts (δ / ppm) for the selected carbons and ^1H - ^{13}C HMQC and HMBC correlations of compound 13f	210
Table 5.18	Chemical shifts (δ / ppm) for the quaternary carbons of compound 13f	211
Table 5.19	Chemical shifts (δ / ppm) for the selected protons of compounds 13a, 13b, 13d, 13e, 13g and 13h	211
Table 5.20	Chemical shifts (δ / ppm) for the selected carbons of compounds 13a, 13b, 13d, 13e, 13g and 13h	212
Table 5.21	The phase transition temperatures ($^{\circ}\text{C}$) and associated enthalpy changes (kJmol^{-1}) of compounds 13a-13h . Only the highest melting points are listed. (\bullet = enantiotropic phase, \circ = monotropic phase, Cr = crystal, SmX = unidentified smectic, SmC* = chiral smectic C, SmA = smectic A, N* = chiral nematic, BP = blue phase, I = isotropic)	214
Table 6.1	C, H and N microanalytical data of compound 14	227

Table 6.2	Selected FT-IR absorption frequency (ν / cm^{-1}) of compound 14	227
Table 6.3	Yields (%) of compounds 15a-15h	230
Table 6.4	C, H and N microanalytical data of compounds 15a-15h	230
Table 6.5	Selected FT-IR absorption frequency (ν / cm^{-1}) of compounds 15a-15h	231
Table 6.6	List of ^1H -NMR chemical shifts (δ / ppm), multiplicity, number of protons and associated functional groups of compounds 15a-15h	237
Table 6.7	Yields (%) of compounds 16a-16h	239
Table 6.8	C, H and N microanalytical data of compounds 16a-16h	239
Table 6.9	Selected FT-IR absorption frequency (ν / cm^{-1}) of compounds 16a-16h	240
Table 6.10	Chemical shifts (δ / ppm) for the selected protons of compound 16e	245
Table 6.11	Chemical shifts (δ / ppm) for the selected carbons and ^1H - ^{13}C HMQC and HMBC correlations of compound 16e	249
Table 6.12	Chemical shifts (δ / ppm) for the quaternary carbons of compound 16e	256
Table 6.13	Chemical shifts (δ / ppm) for the selected protons of compound 16f	257
Table 6.14	Chemical shifts (δ / ppm) for the selected carbons and ^1H - ^{13}C HMQC and HMBC correlations of compound 16f	265
Table 6.15	Chemical shifts (δ / ppm) for the quaternary carbons of compound 16f	268
Table 6.16	Chemical shifts (δ / ppm) for the selected protons of compounds 16a-16d , 16g and 16h	269
Table 6.17	Chemical shifts (δ / ppm) for the selected carbons of compounds 16a-16d , 16g and 16h	269
Table 6.18	Phase transition temperatures ($^{\circ}\text{C}$) and associated enthalpy changes (kJmol^{-1}) of compounds 16a-16h . Only the highest melting points are listed. (\bullet = enantiotropic phase, Cr = crystal, N* = chiral nematic, I = isotropic)	271
Table 7.1	C, H and N microanalytical data of compound 17	275
Table 7.2	Selected FT-IR absorption frequency (ν / cm^{-1}) of compound 17	275
Table 7.3	Yields (%) of compounds 18a-18h	278
Table 7.4	C, H and N microanalytical data of compounds 18a-18h	278

Table 7.5	Selected FT-IR absorption frequency (ν / cm^{-1}) of compounds 18a-18h	281
Table 7.6	List of ^1H -NMR chemical shifts (δ / ppm), multiplicity, number of protons and associated functional groups of compounds 18a-18h	282
Table 7.7	Yields (%) of compounds 19a-19h	286
Table 7.8	C, H and N microanalytical data of compounds 19a-19h	286
Table 7.9	Selected FT-IR absorption frequency (ν / cm^{-1}) of compounds 19a-19h	287
Table 7.10	Chemical shifts (δ / ppm) for the selected protons of compound 19d	292
Table 7.11	Chemical shifts (δ / ppm) for the selected carbons and ^1H - ^{13}C HMQC and HMBC correlations of compound 19d	300
Table 7.12	Chemical shifts (δ / ppm) for the quaternary carbons of compound 19d	303
Table 7.13	Chemical shifts (δ / ppm) for the selected protons of compound 19e	307
Table 7.14	Chemical shifts (δ / ppm) for the selected carbons and ^1H - ^{13}C HMQC and HMBC correlations of compound 19e	309
Table 7.15	Chemical shifts (δ / ppm) for the quaternary carbons of compound 19e	315
Table 7.16	Chemical shifts (δ / ppm) for the selected protons of compounds 19a-19c and 19f-19h	316
Table 7.17	Chemical shifts (δ / ppm) for the selected carbons of compounds 19a-19c and 19f-19h	316
Table 7.18	Phase transition temperatures ($^{\circ}\text{C}$), associated enthalpy changes (kJmol^{-1}) and chiral nematic-isotropic entropy changes of compounds 19a-19h . Only the highest melting points are listed. (\bullet = enantiotropic phase, \circ = monotropic phase, Cr = crystal, N* = chiral nematic, BP = blue phase, I = isotropic)	317
Table 8.1	C, H and N microanalytical data of compounds 23a-23d	329
Table 8.2	Selected FT-IR absorption frequency (ν / cm^{-1}) of compounds 23a-23d	329
Table 8.3	List of ^1H -NMR chemical shifts (δ / ppm), multiplicity, number of protons and associated functional groups of compounds 23a-23d	332
Table 8.4	C, H and N microanalytical data of compounds 24a-24d	336
Table 8.5	Selected FT-IR absorption frequency (ν / cm^{-1}) of compounds 24a-24d	339
Table 8.6	List of ^1H -NMR chemical shifts (δ / ppm), multiplicity, number of protons and associated functional groups of compounds 24a-24d	342

Table 8.7	Yields (%) of compounds 25a-25d and 26a-26d	344
Table 8.8	C, H and N microanalytical data of compounds 25a-25d and 26a-26d	344
Table 8.9	Selected FT-IR absorption frequency (ν / cm^{-1}) of compounds 25a-25d and 26a-26d	345
Table 8.10	Chemical shifts (δ / ppm) for the selected protons of compound 25a	353
Table 8.11	Chemical shifts (δ / ppm) for the selected carbons and ^1H - ^{13}C HMQC and HMBC correlations of compound 25a	355
Table 8.12	Chemical shifts (δ / ppm) for the quaternary carbons of compound 25a	362
Table 8.13	Chemical shifts (δ / ppm) for the selected protons of compound 26c	366
Table 8.14	Chemical shifts (δ / ppm) for the selected carbons and ^1H - ^{13}C HMQC and HMBC correlations of compound 26c	374
Table 8.15	Chemical shifts (δ / ppm) for the quaternary carbons of compound 26c	375
Table 8.16	Chemical shifts (δ / ppm) for the selected protons of compounds 25b , 25c , 25d , 26a , 26b and 26d	376
Table 8.17	Chemical shifts (δ / ppm) for the selected carbons of compounds 25b , 25c , and 25d	377
Table 8.18	Chemical shifts (δ / ppm) for the selected carbons of compounds 26a , 26b , and 26d	378
Table 8.19	Phase transition temperatures ($^{\circ}\text{C}$) and associated enthalpy changes (kJmol^{-1}) of compounds 24a-24d , 25a-25d and 26a-26d . Only the highest melting points are listed. (\bullet = enantiotropic phase, \circ = monotropic phase, T_g = glass transition temperature, Cr = crystal, N = nematic, I = isotropic)	380

LIST OF FIGURES

Figure 1.1	Primary phase transitions and phase transitions involving liquid crystalline phase (in dotted box)	2
Figure 1.2	Nematic phase (Barón, 2001)	3
Figure 1.3	Chiral nematic phase (Barón, 2001)	4
Figure 1.4	Molecular arrangement in (a) SmA phase with Z = optic axis; (b) SmC phase (Barón, 2001)	6
Figure 1.5	SmB phase (Barón, 2001)	7
Figure 1.6	Illustration of the respective tilt directions of the director in the (a) SmF; (b) SmI phases	7
Figure 1.7	SmC* phase with P = helical pitch (Barón, 2001)	8
Figure 1.8	A blue phase model consisting of double-twist cylinders forming a cubic lattice (Barón, 2001)	10
Figure 1.9	Two examples of calamitic mesogens (a) N-[4-(4-octyloxybenzoyloxy)-2-hydroxybenzylidene]-3-aminopyridine (Takase <i>et al.</i> , 2003); (b) 4-[(S)-2-chloro-4-methylpentanoyloxy]-4'-[4-propylbenzoyloxy]-biphenyl (Schacht <i>et al.</i> , 1998)	11
Figure 1.10	Inositol ether (Tschierske, 1998)	11
Figure 1.11	4,6-Dichloro-1,3-phenylenebis[4-(4- <i>n</i> -octyloxyphenyliminomethyl)-benzoate] (Lee <i>et al.</i> , 2003)	12
Figure 1.12	4-Dodecyloxy-2'-(4-butoxybenzoyloxy)-4'-(4-butoxybenzoyloxy)-azobenzenes (Berdagué <i>et al.</i> , 1993)	13
Figure 1.13	Respective example of symmetric dimer and non-symmetric dimer (a) α,ω -bis(4-pentylanilinebenzylidene-4'-oxy)butane (Date <i>et al.</i> , 1992); (b) α -(4-cyanobiphenyl-4'-oxy)- ω -(4-butylanilinebenzylidene-4'-oxy)hexane (Hogan <i>et al.</i> , 1988)	14
Figure 1.14	Structure for the dimer which contains cholesterol and 4-(<i>trans</i> -4- <i>n</i> -hexylcyclohexyl)benzoic acid moieties (Yu <i>et al.</i> , 2008)	14
Figure 1.15	Respective example of symmetric trimer and non-symmetric trimer (a) 4,4'-bis[ω -(4-cyanobiphenyl-4'-yloxy)butyloxy]biphenyl; (b) mesogen incorporating 5-octylpyrimidine-2-yl and 4-cyanophenyl moieties (Yoshizawa <i>et al.</i> , 2005)	15
Figure 2.1	Overall synthetic routes towards obtaining compounds 4a-4j	26

Figure 2.2	Overall synthetic routes towards obtaining compounds 9a-9h	29
Figure 2.3	Overall synthetic routes towards obtaining compounds 13a-13h , 16a-16h and 19a-19h	33
Figure 2.4	Overall synthetic routes towards obtaining compounds 25a-25d and 26a-26d	38
Figure 3.1	Esterification reaction between 4-(4-hydroxyphenyl)benzoic acid and (<i>RS</i>)-2-methyl-1-butanol to yield (<i>RS</i>)-2-methylbutyl-4'-(4''-hydroxyphenyl)benzoate, 1	42
Figure 3.2	Mechanism for the Fischer acid-catalyzed esterification reaction between 4-(4-hydroxyphenyl)benzoic acid and (<i>RS</i>)-2-methyl-1-butanol to yield compound 1	43
Figure 3.3	FT-IR spectrum of (<i>RS</i>)-2-methylbutyl-4'-(4''-hydroxyphenyl)benzoate, 1	45
Figure 3.4	Resonance structure for (<i>RS</i>)-2-methylbutyl-4'-(4''-hydroxyphenyl)benzoate, 1	46
Figure 3.5	Atom numbering for the branched alkyl fragment of compound 1	46
Figure 3.6	¹ H-NMR spectrum of (<i>RS</i>)-2-methylbutyl-4'-(4''-hydroxyphenyl)benzoate, 1	49
Figure 3.7	Condensation reaction between 4-hydroxybenzaldehyde and various 4-substituted-anilines to yield 4-hydroxy-4'-benzylidene-substituted-anilines, 2a-2e	50
Figure 3.8	Mechanism for the condensation reaction between 4-hydroxybenzaldehyde and 4-methylaniline to yield compound 2b	51
Figure 3.9	FT-IR spectrum of 4-hydroxy-4'-benzylidenemethylaniline, 2b and examples of band assignment to the different functional groups	54
Figure 3.10	FT-IR spectrum of 4-hydroxy-4'-benzylidenechloroaniline, 2d	55
Figure 3.11	Atom numbering for the aromatic protons of compound 2	57
Figure 3.12	¹ H-NMR spectrum of 4-hydroxy-4'-benzylidenemethylaniline, 2b and examples of peak assignment to the different types of proton	58
Figure 3.13	¹ H-NMR spectrum of 4-hydroxy-4'-benzylidenechloroaniline, 2d	59
Figure 3.14	Etherification reaction between compounds 2a-2e and 1,6-dibromohexane and 1,8-dibromooctane to yield 4-(<i>n</i> -bromoalkyloxy)-4'-benzylidene-substituted-anilines, 3a-3j	61

Figure 3.15	Mechanism for the Williamson ether synthetic reaction between the phenoxide ion of compound 2b and 1,6-dibromohexane to yield compound 3b	61
Figure 3.16	FT-IR spectrum of 4-(6-bromohexyloxy)-4'-benzylidenemethylaniline, 3b and examples of band assignment to the different functional groups	64
Figure 3.17	FT-IR spectrum of 4-(6-bromohexyloxy)-4'-benzylidenechloroaniline, 3d	65
Figure 3.18	Atom numbering for the aromatic protons of compound 3	67
Figure 3.19	¹ H-NMR spectrum of 4-(6-bromohexyloxy)-4'-benzylidenemethylaniline, 3b and examples of peak assignment to the different types of proton	69
Figure 3.20	¹ H-NMR spectrum of 4-(6-bromohexyloxy)-4'-benzylidenechloroaniline, 3d	70
Figure 3.21	Etherification reaction between compound 1 and compounds 3a-3j to yield α-(4-benzylidene-substituted-aniline-4'-oxy)-ω-[2-methylbutyl-4'-(4''-phenyl)benzoateoxy]alkanes, 4a-4j	72
Figure 3.22	FT-IR spectrum of α-(4-benzylidenemethylaniline-4'-oxy)-ω-[2-methylbutyl-4'-(4''-phenyl)benzoateoxy]hexane, 4b and examples of band assignment to the different functional groups	76
Figure 3.23	FT-IR spectrum of α-(4-benzylidenechloroaniline-4'-oxy)-ω-[2-methylbutyl-4'-(4''-phenyl)benzoateoxy]hexane, 4d	77
Figure 3.24	Atom numbering for compound 4b	78
Figure 3.25	¹ H-NMR spectrum of α-(4-benzylidenemethylaniline-4'-oxy)-ω-[2-methylbutyl-4'-(4''-phenyl)benzoateoxy]hexane, 4b and examples of peak assignment to the different types of proton	79
Figure 3.26	(a) ¹ H- ¹ H COSY spectrum of α-(4-benzylidenemethylaniline-4'-oxy)-ω-[2-methylbutyl-4'-(4''-phenyl)benzoateoxy]hexane, 4b ; (b) representations of some deduced ¹ H- ¹ H COSY correlations	82
Figure 3.27	¹³ C-NMR spectrum of α-(4-benzylidenemethylaniline-4'-oxy)-ω-[2-methylbutyl-4'-(4''-phenyl)benzoateoxy]hexane, 4b	84
Figure 3.28	DEPT 90 spectrum of α-(4-benzylidenemethylaniline-4'-oxy)-ω-[2-methylbutyl-4'-(4''-phenyl)benzoateoxy]hexane, 4b	85
Figure 3.29	DEPT 135 spectrum of α-(4-benzylidenemethylaniline-4'-oxy)-ω-[2-methylbutyl-4'-(4''-phenyl)benzoateoxy]hexane, 4b	86

Figure 3.30	(a) ^1H - ^{13}C HMQC spectrum of α -(4-benzylidenemethylaniline-4'-oxy)- ω -[2-methylbutyl-4'-(4''-phenyl)benzoateoxy]hexane, 4b ; (b) representations of some deduced ^1H - ^{13}C HMQC correlations	87
Figure 3.31	(a) ^1H - ^{13}C HMBC spectrum of α -(4-benzylidenemethylaniline-4'-oxy)- ω -[2-methylbutyl-4'-(4''-phenyl)benzoateoxy]hexane, 4b ; (b) representations of some deduced ^1H - ^{13}C HMBC correlations	89
Figure 3.32	Atom numbering for compound 4d	93
Figure 3.33	^1H -NMR spectrum of α -(4-benzylidenechloroaniline-4'-oxy)- ω -[2-methylbutyl-4'-(4''-phenyl)benzoateoxy]hexane, 4d	94
Figure 3.34	(a) ^1H - ^1H COSY spectrum of α -(4-benzylidenechloroaniline-4'-oxy)- ω -[2-methylbutyl-4'-(4''-phenyl)benzoateoxy]hexane, 4d ; (b) representations of some deduced ^1H - ^1H COSY correlations	95
Figure 3.35	^{13}C -NMR spectrum of α -(4-benzylidenechloroaniline-4'-oxy)- ω -[2-methylbutyl-4'-(4''-phenyl)benzoateoxy]hexane, 4d	98
Figure 3.36	DEPT 90 spectrum of α -(4-benzylidenechloroaniline-4'-oxy)- ω -[2-methylbutyl-4'-(4''-phenyl)benzoateoxy]hexane, 4d	99
Figure 3.37	DEPT 135 spectrum of α -(4-benzylidenechloroaniline-4'-oxy)- ω -[2-methylbutyl-4'-(4''-phenyl)benzoateoxy]hexane, 4d	100
Figure 3.38	(a) ^1H - ^{13}C HMQC spectrum of α -(4-benzylidenechloroaniline-4'-oxy)- ω -[2-methylbutyl-4'-(4''-phenyl)benzoateoxy]hexane, 4d ; (b) representations of some deduced ^1H - ^{13}C HMQC correlations	101
Figure 3.39	(a) ^1H - ^{13}C HMBC spectrum of α -(4-benzylidenechloroaniline-4'-oxy)- ω -[2-methylbutyl-4'-(4''-phenyl)benzoateoxy]hexane, 4d ; (b) representations of some deduced ^1H - ^{13}C HMBC correlations	102
Figure 3.40	DSC trace of compound 4c on heating and cooling cycles at the rate of $\pm 2\text{ }^\circ\text{Cmin}^{-1}$	110
Figure 3.41	Schlieren texture of the nematic phase of compound 4i at $131.4\text{ }^\circ\text{C}$	111
Figure 3.42	Focal conic fan texture containing polygonal defects of the SmA phase of compound 4e at $114.5\text{ }^\circ\text{C}$	111
Figure 3.43	Derived intensity versus 2θ profile of the X-ray diffraction powder pattern of compound 4e in the intercalated SmA phase at $110\text{ }^\circ\text{C}$. The inset shows the intensity versus 2θ profile in the Cr phase at $100\text{ }^\circ\text{C}$.	113
Figure 3.44	Sketch of the molecular organization within the intercalated SmA phase shown by 4e . The layer periodicity is indicated as 18.3 \AA .	114

Figure 4.1	Esterification reaction between 4-hydroxybenzaldehyde and 2-thiophenecarbonyl chloride to yield 4-formylphenyl thiophene-2-carboxylate, 5	118
Figure 4.2	Mechanism for the Schotten-Baumann esterification reaction between 4-hydroxybenzaldehyde and 2-thiophenecarbonyl chloride to yield compound 5	119
Figure 4.3	FT-IR spectrum of 4-formylphenyl thiophene-2-carboxylate, 5	122
Figure 4.4	¹ H-NMR spectrum of 4-formylphenyl thiophene-2-carboxylate, 5	123
Figure 4.5	Condensation reaction between 4-aminophenol and compound 5 to yield 4-(thiophene-2-carboxyl)benzylidene-4'-hydroxyaniline, 6	124
Figure 4.6	FT-IR spectrum of 4-(thiophene-2-carboxyl)benzylidene-4'-hydroxyaniline, 6	128
Figure 4.7	¹ H-NMR spectrum of 4-(thiophene-2-carboxyl)benzylidene-4'-hydroxyaniline, 6	129
Figure 4.8	Etherification reaction between compound 7 and a series of α,ω -dibromoalkanes to yield 4-(<i>n</i> -bromoalkyloxy)-4'-benzylidenechloroanilines, 8a-8h	130
Figure 4.9	FT-IR spectrum of 4-(7-bromoheptyloxy)-4'-benzylidenechloroaniline, 8c	132
Figure 4.10	¹ H-NMR spectrum of 4-(7-bromoheptyloxy)-4'-benzylidenechloroaniline, 8c	134
Figure 4.11	Etherification reaction between compound 6 and compounds 8a-8h to yield α -(4-benzylidenechloroaniline-4'-oxy)- ω -[4-(thiophene-2-carboxyl)benzylideneaniline-4'-oxy]alkanes, 9a-9h	136
Figure 4.12	FT-IR spectrum of α -(4-benzylidenechloroaniline-4'-oxy)- ω -[4-(thiophene-2-carboxyl)benzylideneaniline-4'-oxy]heptane, 9c	139
Figure 4.13	Atom numbering for compound 9c	140
Figure 4.14	¹ H-NMR spectrum of α -(4-benzylidenechloroaniline-4'-oxy)- ω -[4-(thiophene-2-carboxyl)benzylideneaniline-4'-oxy]heptane, 9c	143
Figure 4.15	(a) ¹ H- ¹ H COSY spectrum of α -(4-benzylidenechloroaniline-4'-oxy)- ω -[4-(thiophene-2-carboxyl)benzylideneaniline-4'-oxy]heptane, 9c ; (b) representations of some deduced ¹ H- ¹ H COSY correlations	144
Figure 4.16	¹³ C-NMR spectrum of α -(4-benzylidenechloroaniline-4'-oxy)- ω -[4-(thiophene-2-carboxyl)benzylideneaniline-4'-oxy]heptane, 9c	146

Figure 4.17	DEPT 90 spectrum of α -(4-benzylidenechloroaniline-4'-oxy)- ω -[4-(thiophene-2-carboxyl)benzylideneaniline-4'-oxy]heptane, 9c	147
Figure 4.18	DEPT 135 spectrum of α -(4-benzylidenechloroaniline-4'-oxy)- ω -[4-(thiophene-2-carboxyl)benzylideneaniline-4'-oxy]heptane, 9c	148
Figure 4.19	(a) ^1H - ^{13}C HMQC spectrum of α -(4-benzylidenechloroaniline-4'-oxy)- ω -[4-(thiophene-2-carboxyl)benzylideneaniline-4'-oxy]heptane, 9c ; (b) representations of some deduced ^1H - ^{13}C HMQC correlations	152
Figure 4.20	(a) ^1H - ^{13}C HMBC spectrum of α -(4-benzylidenechloroaniline-4'-oxy)- ω -[4-(thiophene-2-carboxyl)benzylideneaniline-4'-oxy]heptane, 9c ; (b) representations of some deduced ^1H - ^{13}C HMBC correlations	153
Figure 4.21	Dependence of phase transition temperatures, T on the number of methylene units, <i>n</i> in the flexible spacer	159
Figure 4.22	Comparison of N phase temperature range, T between odd and even members during heating run	159
Figure 4.23	DSC trace of compound 9d with heating and cooling rates of $\pm 5\text{ }^\circ\text{Cmin}^{-1}$	160
Figure 4.24	Dependence of the entropy change ($\Delta S_{\text{NI}}/R$) associated with the nematic-isotropic transition on the number of methylene units, <i>n</i> in the flexible spacer	161
Figure 4.25	N schlieren texture (compound 9g) with both twofold and fourfold brushes at 186.0 $^\circ\text{C}$	162
Figure 4.26	Filaments observed in the homeotropic region of N phase (compound 9f) which initially form (left) upon cooling and gradually transform to compact domain (right)	163
Figure 5.1	Esterification reaction between 4-(4-hydroxyphenyl)benzoic acid and (<i>S</i>)-(-)-2-methyl-1-butanol to yield (<i>S</i>)-(-)-2-methylbutyl-4'-(4''-hydroxyphenyl)benzoate, 10	164
Figure 5.2	FT-IR spectrum of (<i>S</i>)-(-)-2-methylbutyl-4'-(4''-hydroxyphenyl)benzoate, 10	167
Figure 5.3	^1H -NMR spectrum of (<i>S</i>)-(-)-2-methylbutyl-4'-(4''-hydroxyphenyl)benzoate, 10	168
Figure 5.4	Condensation reaction between 1,4-diaminobenzene and 4-hydroxybenzaldehyde to yield 4,4'-bis(4-hydroxybenzylidene)-1,4-diaminobenzene, 11	169
Figure 5.5	FT-IR spectrum of 4,4'-bis(4-hydroxybenzylidene)-1,4-diaminobenzene, 11	171

Figure 5.6	Etherification reaction between compound 11 and a series of α,ω -dibromoalkanes to yield 4,4'-bis[4-(<i>n</i> -bromoalkoxy)benzylidene]-1,4-diaminobenzenes, 12a-12h	172
Figure 5.7	FT-IR spectrum of 4,4'-bis[4-(7-bromoheptyloxy)benzylidene]-1,4-diaminobenzene, 12c	175
Figure 5.8	FT-IR spectrum of 4,4'-bis[4-(10-bromodecyloxy)benzylidene]-1,4-diaminobenzene, 12f	176
Figure 5.9	^1H -NMR spectrum of 4,4'-bis[4-(7-bromoheptyloxy)benzylidene]-1,4-diaminobenzene, 12c	178
Figure 5.10	^1H -NMR spectrum of 4,4'-bis[4-(10-bromodecyloxy)benzylidene]-1,4-diaminobenzene, 12f	179
Figure 5.11	Etherification reaction between compound 10 and compounds 12a-12h to yield 4,4'-bis{ ω -[2-methylbutyl-4'-(4''-phenyl)benzoateoxy]-alkyloxybenzylidene}-1,4-diaminobenzenes, 13a-13h	181
Figure 5.12	FT-IR spectrum of 4,4'-bis{ ω -[2-methylbutyl-4'-(4''-phenyl)benzoateoxy]heptyloxybenzylidene}-1,4-diaminobenzene, 13c	183
Figure 5.13	FT-IR spectrum of 4,4'-bis{ ω -[2-methylbutyl-4'-(4''-phenyl)benzoateoxy]decyloxybenzylidene}-1,4-diaminobenzene, 13f	184
Figure 5.14	Atom numbering for compound 13c	185
Figure 5.15	^1H -NMR spectrum of 4,4'-bis{ ω -[2-methylbutyl-4'-(4''-phenyl)benzoateoxy]heptyloxybenzylidene}-1,4-diaminobenzene, 13c	188
Figure 5.16	(a) ^1H - ^1H COSY spectrum of 4,4'-bis{ ω -[2-methylbutyl-4'-(4''-phenyl)benzoateoxy]heptyloxybenzylidene}-1,4-diaminobenzene, 13c ; (b) representations of some deduced ^1H - ^1H COSY correlations	189
Figure 5.17	^{13}C -NMR spectrum of 4,4'-bis{ ω -[2-methylbutyl-4'-(4''-phenyl)benzoateoxy]heptyloxybenzylidene}-1,4-diaminobenzene, 13c	192
Figure 5.18	DEPT 90 spectrum of 4,4'-bis{ ω -[2-methylbutyl-4'-(4''-phenyl)benzoateoxy]heptyloxybenzylidene}-1,4-diaminobenzene, 13c	193
Figure 5.19	DEPT 135 spectrum of 4,4'-bis{ ω -[2-methylbutyl-4'-(4''-phenyl)benzoateoxy]heptyloxybenzylidene}-1,4-diaminobenzene, 13c	194
Figure 5.20	(a) ^1H - ^{13}C HMQC spectrum of 4,4'-bis{ ω -[2-methylbutyl-4'-(4''-phenyl)benzoateoxy]heptyloxybenzylidene}-1,4-diaminobenzene, 13c ; (b) representations of some deduced ^1H - ^{13}C HMQC correlations	195
Figure 5.21	(a) ^1H - ^{13}C HMBC spectrum of 4,4'-bis{ ω -[2-methylbutyl-4'-(4''-phenyl)benzoateoxy]heptyloxybenzylidene}-1,4-diaminobenzene, 13c ; (b) representations of some deduced ^1H - ^{13}C HMBC correlations	197

Figure 5.22	Atom numbering for compound 13f	198
Figure 5.23	^1H -NMR spectrum of 4,4'-bis{ ω -[2-methylbutyl-4'-(4''-phenyl)-benzoateoxy]decyloxybenzylidene}-1,4-diaminobenzene, 13f	200
Figure 5.24	(a) ^1H - ^1H COSY spectrum of 4,4'-bis{ ω -[2-methylbutyl-4'-(4''-phenyl)benzoateoxy]decyloxybenzylidene}-1,4-diaminobenzene, 13f ; (b) representations of some deduced ^1H - ^1H COSY correlations	201
Figure 5.25	^{13}C -NMR spectrum of 4,4'-bis{ ω -[2-methylbutyl-4'-(4''-phenyl)-benzoateoxy]decyloxybenzylidene}-1,4-diaminobenzene, 13f	205
Figure 5.26	DEPT 90 spectrum of 4,4'-bis{ ω -[2-methylbutyl-4'-(4''-phenyl)-benzoateoxy]decyloxybenzylidene}-1,4-diaminobenzene, 13f	206
Figure 5.27	DEPT 135 spectrum of 4,4'-bis{ ω -[2-methylbutyl-4'-(4''-phenyl)-benzoateoxy]decyloxybenzylidene}-1,4-diaminobenzene, 13f	207
Figure 5.28	(a) ^1H - ^{13}C HMQC spectrum of 4,4'-bis{ ω -[2-methylbutyl-4'-(4''-phenyl)benzoateoxy]decyloxybenzylidene}-1,4-diaminobenzene, 13f ; (b) representations of some deduced ^1H - ^{13}C HMQC correlations	208
Figure 5.29	(a) ^1H - ^{13}C HMBC spectrum of 4,4'-bis{ ω -[2-methylbutyl-4'-(4''-phenyl)benzoateoxy]decyloxybenzylidene}-1,4-diaminobenzene, 13f ; (b) representations of some deduced ^1H - ^{13}C HMBC correlations	209
Figure 5.30	Dependence of the transition temperatures on the number of methylene units, n in the flexible spacers for compounds 13a-13h	215
Figure 5.31	DSC trace of compound 13a with heating and cooling rate of $\pm 5\text{ }^\circ\text{Cmin}^{-1}$	215
Figure 5.32	SmA fan-shaped texture of compound 13d at 198.2 $^\circ\text{C}$ upon heating	217
Figure 5.33	Dependence of smectic layer spacing on temperature for	
	(a) compound 13a	217
	(b) compound 13c	218
	(c) compound 13e	218
	(d) compound 13f and	219
	(e) compound 13g	219
Figure 5.34	Photomicrograph of the monotropic SmF* mosaic-schlieren texture of compound 13c upon cooling the SmC* phase	222
Figure 5.35	Evolution from	
	(a) the SmA homeotropic texture at 164.4 $^\circ\text{C}$ to	222
	(b) pseudo-homeotropic texture of the SmC* phase at 152.0 $^\circ\text{C}$ to	222
	(c) the coexistence of homeotropic and platelet / fan-like texture of the SmX phase at 136.0 $^\circ\text{C}$	222

Figure 5.36	Mosaic texture of the monotropic SmX phase of compound 13e	223
Figure 5.37	Proposed conformation of 13f based on MM2 minimum energetic parameters	223
Figure 5.38	Proposed SmA ₁ molecular organization model for compound 13f with layer spacing of 72.6 Å	224
Figure 5.39	Platelet texture of the blue phase (compound 13e) upon cooling the isotropic phase	225
Figure 6.1	Condensation reaction between 1,4-diaminobenzene and vanillin to yield 4,4'-bis(3-methoxy-4-hydroxybenzylidene)-1,4-diaminobenzene, 14	226
Figure 6.2	FT-IR spectrum of 4,4'-bis(3-methoxy-4-hydroxybenzylidene)-1,4-diaminobenzene, 14	228
Figure 6.3	Etherification reaction between compound 14 and a series of α,ω -dibromoalkanes to yield 4,4'-bis[3-methoxy-4-(<i>n</i> -bromoalkyloxy)-benzylidene]-1,4-diaminobenzenes, 15a-15h	229
Figure 6.4	FT-IR spectrum of 4,4'-bis[3-methoxy-4-(9-bromononyloxy)-benzylidene]-1,4-diaminobenzene, 15e	232
Figure 6.5	FT-IR spectrum of 4,4'-bis[3-methoxy-4-(10-bromodecyloxy)-benzylidene]-1,4-diaminobenzene, 15f	233
Figure 6.6	¹ H-NMR spectrum of 4,4'-bis[3-methoxy-4-(9-bromononyloxy)-benzylidene]-1,4-diaminobenzene, 15e	235
Figure 6.7	¹ H-NMR spectrum of 4,4'-bis[3-methoxy-4-(10-bromodecyloxy)-benzylidene]-1,4-diaminobenzene, 15f	236
Figure 6.8	Etherification reaction between compound 10 and compounds 15a-15h to yield 4,4'-bis{ ω -[2-methylbutyl-4'-(4''-phenyl)-benzoateoxy]-3-methoxy-4-alkyloxybenzylidene}-1,4-diaminobenzenes, 16a-16h	238
Figure 6.9	FT-IR spectrum of 4,4'-bis{ ω -[2-methylbutyl-4'-(4''-phenyl)-benzoateoxy]-3-methoxy-4-nonyloxybenzylidene}-1,4-diaminobenzene, 16e	241
Figure 6.10	FT-IR spectrum of 4,4'-bis{ ω -[2-methylbutyl-4'-(4''-phenyl)-benzoateoxy]-3-methoxy-4-decyloxybenzylidene}-1,4-diaminobenzene, 16f	242
Figure 6.11	Atom numbering for compound 16e	243

Figure 6.12	^1H -NMR spectrum of 4,4'-bis{ ω -[2-methylbutyl-4'-(4''-phenyl)-benzoateoxy]-3-methoxy-4-nonyloxybenzylidene}-1,4-diaminobenzene, 16e	246
Figure 6.13	(a) ^1H - ^1H COSY spectrum of 4,4'-bis{ ω -[2-methylbutyl-4'-(4''-phenyl)benzoateoxy]-3-methoxy-4-nonyloxybenzylidene}-1,4-diaminobenzene, 16e ; (b) representations of some deduced ^1H - ^1H COSY correlations	247
Figure 6.14	^{13}C -NMR spectrum of 4,4'-bis{ ω -[2-methylbutyl-4'-(4''-phenyl)-benzoateoxy]-3-methoxy-4-nonyloxybenzylidene}-1,4-diaminobenzene, 16e	250
Figure 6.15	DEPT 90 spectrum of 4,4'-bis{ ω -[2-methylbutyl-4'-(4''-phenyl)-benzoateoxy]-3-methoxy-4-nonyloxybenzylidene}-1,4-diaminobenzene, 16e	251
Figure 6.16	DEPT 135 spectrum of 4,4'-bis{ ω -[2-methylbutyl-4'-(4''-phenyl)-benzoateoxy]-3-methoxy-4-nonyloxybenzylidene}-1,4-diaminobenzene, 16e	252
Figure 6.17	(a) ^1H - ^{13}C HMQC spectrum of 4,4'-bis{ ω -[2-methylbutyl-4'-(4''-phenyl)benzoateoxy]-3-methoxy-4-nonyloxybenzylidene}-1,4-diaminobenzene, 16e ; (b) representations of some deduced ^1H - ^{13}C HMQC correlations	253
Figure 6.18	(a) ^1H - ^{13}C HMBC spectrum of 4,4'-bis{ ω -[2-methylbutyl-4'-(4''-phenyl)benzoateoxy]-3-methoxy-4-nonyloxybenzylidene}-1,4-diaminobenzene, 16e ; (b) representations of some deduced ^1H - ^{13}C HMBC correlations	255
Figure 6.19	Atom numbering for compound 16f	256
Figure 6.20	^1H -NMR spectrum of 4,4'-bis{ ω -[2-methylbutyl-4'-(4''-phenyl)-benzoateoxy]-3-methoxy-4-decyloxybenzylidene}-1,4-diaminobenzene, 16f	258
Figure 6.21	(a) ^1H - ^1H COSY spectrum of 4,4'-bis{ ω -[2-methylbutyl-4'-(4''-phenyl)benzoateoxy]-3-methoxy-4-decyloxybenzylidene}-1,4-diaminobenzene, 16f ; (b) representations of some deduced ^1H - ^1H COSY correlations	259
Figure 6.22	^{13}C -NMR spectrum of 4,4'-bis{ ω -[2-methylbutyl-4'-(4''-phenyl)benzoateoxy]-3-methoxy-4-decyloxybenzylidene}-1,4-diaminobenzene, 16f	261
Figure 6.23	DEPT 90 spectrum of 4,4'-bis{ ω -[2-methylbutyl-4'-(4''-phenyl)benzoateoxy]-3-methoxy-4-decyloxybenzylidene}-1,4-diaminobenzene, 16f	262

Figure 6.24	DEPT 135 spectrum of 4,4'-bis{ω-[2-methylbutyl-4'-(4''-phenyl)benzoateoxy]-3-methoxy-4-decyloxybenzylidene}-1,4-diaminobenzene, 16f	263
Figure 6.25	(a) ¹ H- ¹³ C HMQC spectrum of 4,4'-bis{ω-[2-methylbutyl-4'-(4''-phenyl)benzoateoxy]-3-methoxy-4-decyloxybenzylidene}-1,4-diaminobenzene, 16f ; (b) representations of some deduced ¹ H- ¹³ C HMQC correlations	264
Figure 6.26	(a) ¹ H- ¹³ C HMBC spectrum of 4,4'-bis{ω-[2-methylbutyl-4'-(4''-phenyl)benzoateoxy]-3-methoxy-4-decyloxybenzylidene}-1,4-diaminobenzene, 16f ; (b) representations of some deduced ¹ H- ¹³ C HMBC correlations	267
Figure 6.27	Photomicrograph of fluid oily streaks in the N* domains upon the heating run prior to N*-I transition (compound 16b)	272
Figure 6.28	Photomicrograph of N* phase exhibiting violet / blue iridescent colours in formation of oily streaks texture (compound 16d)	272
Figure 7.1	Condensation reaction between 1,4-diaminobenzene and 3-bromo-4-hydroxybenzaldehyde to yield 4,4'-bis(3-bromo-4-hydroxybenzylidene)-1,4-diaminobenzene, 17	274
Figure 7.2	FT-IR spectrum of 4,4'-bis(3-bromo-4-hydroxybenzylidene)-1,4-diaminobenzene, 17	276
Figure 7.3	Etherification reaction between compound 17 and a series of α,ω-dibromoalkanes to yield 4,4'-bis[3-bromo-4-(<i>n</i> -bromoalkyloxy)benzylidene]-1,4-diaminobenzenes, 18a-18h	277
Figure 7.4	FT-IR spectrum of 4,4'-bis[3-bromo-4-(8-bromooctyloxy)benzylidene]-1,4-diaminobenzene, 18d	279
Figure 7.5	FT-IR spectrum of 4,4'-bis[3-bromo-4-(9-bromononyloxy)benzylidene]-1,4-diaminobenzene, 18e	280
Figure 7.6	¹ H-NMR spectrum of 4,4'-bis[3-bromo-4-(8-bromooctyloxy)benzylidene]-1,4-diaminobenzene, 18d	283
Figure 7.7	¹ H-NMR spectrum of 4,4'-bis[3-bromo-4-(9-bromononyloxy)benzylidene]-1,4-diaminobenzene, 18e	284
Figure 7.8	Etherification reaction between compound 10 and compounds 18a-18h to yield 4,4'-bis{ω-[2-methylbutyl-4'-(4''-phenyl)benzoateoxy]-3-bromo-4-alkyloxybenzylidene}-1,4-diaminobenzenes, 19a-19h	285
Figure 7.9	FT-IR spectrum of 4,4'-bis{ω-[2-methylbutyl-4'-(4''-phenyl)benzoateoxy]-3-bromo-4-octyloxybenzylidene}-1,4-diaminobenzene, 19d	288

Figure 7.10	FT-IR spectrum of 4,4'-bis{ω-[2-methylbutyl-4'-(4''-phenyl)-benzoateoxy]-3-bromo-4-nonyloxybenzylidene}-1,4-diaminobenzene, 19e	289
Figure 7.11	Atom numbering for compound 19d	290
Figure 7.12	¹ H-NMR spectrum of 4,4'-bis{ω-[2-methylbutyl-4'-(4''-phenyl)-benzoateoxy]-3-bromo-4-octyloxybenzylidene}-1,4-diaminobenzene, 19d	294
Figure 7.13	(a) ¹ H- ¹ H COSY spectrum of 4,4'-bis{ω-[2-methylbutyl-4'-(4''-phenyl)benzoateoxy]-3-bromo-4-octyloxybenzylidene}-1,4-diaminobenzene, 19d ; (b) representations of some deduced ¹ H- ¹ H COSY correlations	295
Figure 7.14	¹³ C-NMR spectrum of 4,4'-bis{ω-[2-methylbutyl-4'-(4''-phenyl)-benzoateoxy]-3-bromo-4-octyloxybenzylidene}-1,4-diaminobenzene, 19d	296
Figure 7.15	DEPT 90 spectrum of 4,4'-bis{ω-[2-methylbutyl-4'-(4''-phenyl)-benzoateoxy]-3-bromo-4-octyloxybenzylidene}-1,4-diaminobenzene, 19d	297
Figure 7.16	DEPT 135 spectrum of 4,4'-bis{ω-[2-methylbutyl-4'-(4''-phenyl)-benzoateoxy]-3-bromo-4-octyloxybenzylidene}-1,4-diaminobenzene, 19d	298
Figure 7.17	(a) ¹ H- ¹³ C HMQC spectrum of 4,4'-bis{ω-[2-methylbutyl-4'-(4''-phenyl)benzoateoxy]-3-bromo-4-octyloxybenzylidene}-1,4-diaminobenzene, 19d ; (b) representations of some deduced ¹ H- ¹³ C HMQC correlations	299
Figure 7.18	(a) ¹ H- ¹³ C HMBC spectrum of 4,4'-bis{ω-[2-methylbutyl-4'-(4''-phenyl)benzoateoxy]-3-bromo-4-octyloxybenzylidene}-1,4-diaminobenzene, 19d ; (b) representations of some deduced ¹ H- ¹³ C HMBC correlations	301
Figure 7.19	Atom numbering for compound 19e	303
Figure 7.20	¹ H-NMR spectrum of 4,4'-bis{ω-[2-methylbutyl-4'-(4''-phenyl)-benzoateoxy]-3-bromo-4-nonyloxybenzylidene}-1,4-diaminobenzene, 19e	305
Figure 7.21	(a) ¹ H- ¹ H COSY spectrum of 4,4'-bis{ω-[2-methylbutyl-4'-(4''-phenyl)benzoateoxy]-3-bromo-4-nonyloxybenzylidene}-1,4-diaminobenzene, 19e ; (b) representations of some deduced ¹ H- ¹ H COSY correlations	306
Figure 7.22	¹³ C-NMR spectrum of 4,4'-bis{ω-[2-methylbutyl-4'-(4''-phenyl)-benzoateoxy]-3-bromo-4-nonyloxybenzylidene}-1,4-diaminobenzene, 19e	310

Figure 7.23	DEPT 90 spectrum of 4,4'-bis{ω-[2-methylbutyl-4'-(4''-phenyl)-benzoateoxy]-3-bromo-4-nonyloxybenzylidene}-1,4-diaminobenzene, 19e	311
Figure 7.24	DEPT 135 spectrum of 4,4'-bis{ω-[2-methylbutyl-4'-(4''-phenyl)-benzoateoxy]-3-bromo-4-nonyloxybenzylidene}-1,4-diaminobenzene, 19e	312
Figure 7.25	(a) ^1H - ^{13}C HMQC spectrum of 4,4'-bis{ω-[2-methylbutyl-4'-(4''-phenyl)benzoateoxy]-3-bromo-4-nonyloxybenzylidene}-1,4-diaminobenzene, 19e ; (b) representations of some deduced ^1H - ^{13}C HMQC correlations	313
Figure 7.26	(a) ^1H - ^{13}C HMBC spectrum of 4,4'-bis{ω-[2-methylbutyl-4'-(4''-phenyl)benzoateoxy]-3-bromo-4-nonyloxybenzylidene}-1,4-diaminobenzene, 19e ; (b) representations of some deduced ^1H - ^{13}C HMBC correlations	314
Figure 7.27	Dependence of the transition temperatures on the number of methylene units, n in the flexible spacers for compounds 19a-19h	318
Figure 7.28	Dependence of chiral nematic-isotropic transitional entropy, $\Delta S_{\text{N}^*\text{I}}/\text{R}$ on the number of methylene units, n in the flexible spacers for compounds 19b-19f and 19h	321
Figure 7.29	N* oily streaks texture of compound 19b at 170.1 °C upon heating	321
Figure 7.30	Comparison of N*-I transition temperatures among trimers from three series; compounds 13a-13h , 16b , 16d , 16f and 16h and 19b-19f and 19h	323
Figure 7.31	Photomicrograph showing the blue phase-N* transition upon cooling of compound 19c	324
Figure 7.32	DSC trace for compound 19c with ± 5 °Cmin $^{-1}$ heating and cooling rates	324
Figure 8.1	Condensation reaction between 4-hydroxybenzaldehyde and 4-substituted-anilines with terminal Cl or Br atom to yield 4-hydroxy-4'-benzylidenechloroaniline, 22a and 4-hydroxy-4'-benzylidenebromoaniline, 22b , respectively	325
Figure 8.2	FT-IR spectrum of 4-hydroxy-4'-benzylidenebromoaniline, 22b	326
Figure 8.3	^1H -NMR spectrum of 4-hydroxy-4'-benzylidenebromoaniline, 22b	327
Figure 8.4	Etherification reaction between compounds 22a , 22b and 1,4-dibromobutane and 1,6-dibromohexane to yield 4-(n -bromoalkyloxy)-4'-benzylidene-substituted-anilines, 23a-23d	328

Figure 8.5	FT-IR spectrum of 4-(4-bromobutyloxy)-4'-benzylidenechloroaniline, 23a	333
Figure 8.6	FT-IR spectrum of 4-(4-bromobutyloxy)-4'-benzylidenebromoaniline, 23c	334
Figure 8.7	¹ H-NMR spectrum of 4-(4-bromobutyloxy)-4'-benzylidenechloroaniline, 23a	336
Figure 8.8	¹ H-NMR spectrum of 4-(4-bromobutyloxy)-4'-benzylidenebromoaniline, 23c	337
Figure 8.9	Etherification reaction between 2,4-dihydroxybenzaldehyde and compounds 23a-23d to yield benzyl-2,4-oxybis(4'-halogenoanilinebenzylidene-4''-oxy)alkane aldehydes, 24a-24d	338
Figure 8.10	FT-IR spectrum of benzyl-2,4-oxybis(4'-chloroanilinebenzylidene-4''-oxy)butane aldehyde, 24a	340
Figure 8.11	FT-IR spectrum of benzyl-2,4-oxybis(4'-bromoanilinebenzylidene-4''-oxy)butane aldehyde, 24c	341
Figure 8.12	¹ H-NMR spectrum of benzyl-2,4-oxybis(4'-chloroanilinebenzylidene-4''-oxy)butane aldehyde, 24a	343
Figure 8.13	¹ H-NMR spectrum of benzyl-2,4-oxybis(4'-bromoanilinebenzylidene-4''-oxy)butane aldehyde, 24c	344
Figure 8.14	Condensation reaction between compounds 24a-24d and corresponding 4-substituted-anilines to yield 4-ethyl- and 4-fluoroanilinebenzylidene-2',4'-oxybis(4''-halogenoanilinebenzylidene-4'''-oxy)alkanes, 25a-25d and 26a-26d	346
Figure 8.15	FT-IR spectrum of 4-ethylanilinebenzylidene-2',4'-oxybis(4''-chloroanilinebenzylidene-4'''-oxy)butane, 25a	349
Figure 8.16	FT-IR spectrum of 4-fluoroanilinebenzylidene-2',4'-oxybis(4''-bromoanilinebenzylidene-4'''-oxy)butane, 26c	350
Figure 8.17	Atom numbering for compound 25a	351
Figure 8.18	¹ H-NMR spectrum of 4-ethylanilinebenzylidene-2',4'-oxybis(4''-chloroanilinebenzylidene-4'''-oxy)butane, 25a	354
Figure 8.19	(a) ¹ H- ¹ H COSY spectrum of 4-ethylanilinebenzylidene-2',4'-oxybis(4''-chloroanilinebenzylidene-4'''-oxy)butane, 25a ; (b) representations of some deduced ¹ H- ¹ H COSY correlations	355
Figure 8.20	¹³ C-NMR spectrum of 4-ethylanilinebenzylidene-2',4'-oxybis(4''-chloroanilinebenzylidene-4'''-oxy)butane, 25a	360

Figure 8.21	DEPT 90 spectrum of 4-ethylanilinebenzylidene-2',4'-oxybis(4''-chloroanilinebenzylidene-4'''-oxy)butane, 25a	361
Figure 8.22	DEPT 135 spectrum of 4-ethylanilinebenzylidene-2',4'-oxybis(4''-chloroanilinebenzylidene-4'''-oxy)butane, 25a	362
Figure 8.23	(a) ^1H - ^{13}C HMQC spectrum of 4-ethylanilinebenzylidene-2',4'-oxybis(4''-chloroanilinebenzylidene-4'''-oxy)butane, 25a ; (b) representations of some deduced ^1H - ^{13}C HMQC correlations	363
Figure 8.24	(a) ^1H - ^{13}C HMBC spectrum of 4-ethylanilinebenzylidene-2',4'-oxybis(4''-chloroanilinebenzylidene-4'''-oxy)butane, 25a ; (b) representations of some deduced ^1H - ^{13}C HMBC correlations	364
Figure 8.25	Atom numbering for compound 26c	365
Figure 8.26	^1H -NMR spectrum of 4-fluoroanilinebenzylidene-2',4'-oxybis(4''-bromoanilinebenzylidene-4'''-oxy)butane, 26c	367
Figure 8.27	(a) ^1H - ^1H COSY spectrum of 4-fluoroanilinebenzylidene-2',4'-oxybis(4''-bromoanilinebenzylidene-4'''-oxy)butane, 26c ; (b) representations of some deduced ^1H - ^1H COSY correlations	368
Figure 8.28	^{13}C -NMR spectrum of 4-fluoroanilinebenzylidene-2',4'-oxybis(4''-bromoanilinebenzylidene-4'''-oxy)butane, 26c	371
Figure 8.29	DEPT 90 spectrum of 4-fluoroanilinebenzylidene-2',4'-oxybis(4''-bromoanilinebenzylidene-4'''-oxy)butane, 26c	372
Figure 8.30	DEPT 135 spectrum of 4-fluoroanilinebenzylidene-2',4'-oxybis(4''-bromoanilinebenzylidene-4'''-oxy)butane, 26c	373
Figure 8.31	(a) ^1H - ^{13}C HMQC spectrum of 4-fluoroanilinebenzylidene-2',4'-oxybis(4''-bromoanilinebenzylidene-4'''-oxy)butane, 26c ; (b) representations of some deduced ^1H - ^{13}C HMQC correlations	374
Figure 8.32	(a) ^1H - ^{13}C HMBC spectrum of 4-fluoroanilinebenzylidene-2',4'-oxybis(4''-bromoanilinebenzylidene-4'''-oxy)butane, 26c ; (b) representations of some deduced ^1H - ^{13}C HMBC correlations	376
Figure 8.33	DSC trace of compound 25a with heat capacity change of $0.4 \text{ kJ}(\text{mol}\cdot^\circ\text{C})^{-1}$ at 13.4°C . G indicates the glassy state. The heat capacity change is observed at G-N phase transition upon second heating.	382
Figure 8.34	DSC trace of compound 25b with heat capacity change of $0.3 \text{ kJ}(\text{mol}\cdot^\circ\text{C})^{-1}$ at 5.2°C . G indicates the glassy state. The heat capacity change is observed at G-N phase transition upon second heating.	384
Figure 8.35	Plot of phase temperature ($^\circ\text{C}$) range upon cooling for compounds 24a-24d (* denotes mp)	385

Figure 8.36	Plot of phase temperature (°C) range upon cooling for fluorinated compounds 26a-26d (* denotes mp)	386
Figure 8.37	Powder X-ray diffraction profile for compound 25c in the nematic phase at 120.0 °C. The red curve indicates that the signal fits the Lorentzian function	389
Figure 8.38	Proposed MM2 optimized structure of 25c based on minimum energetic parameters. The estimated length of the trimer is 40 Å.	389
Figure 8.39	Nematic schlieren texture with twofold and fourfold brushes of compound 25d at 117.8 °C upon cooling	391

SINTESIS DAN SIFAT MESOMORFIK BAGI OLIGOMER PELBAGAI-FUNGSIAN BERSIMETRI DAN BUKAN-SIMETRI

ABSTRAK

Enam siri oligomer bersimetri dan tidak bersimetri dengan pelbagai kumpulan berfungsi telah disintesis dan dicirikan. Oligomer ini terdiri daripada dua siri dimer tidak bersimetri, tiga siri trimer bersimetri dan satu siri trimer tidak bersimetri. Siri pertama dimer tidak bersimetri, α -(4-benzilidina-tertutukarganti-anilina-4'-oksi)- ω -[2-metilbutil-4'-(4''-fenil)benzoatoksi]alkana terdiri daripada sepuluh homolog yang berbeza dari segi kumpulan tertutukarganti, X = H, CH₃, F, Cl and Br dan juga spaser C₆H₁₂ and C₈H₁₆. Dimer ini mempamerkan fasa nematik enantiotropik kecuali sebatian dengan X = H. Kedua-dua dimer dengan atom tertutukarganti Br juga mempamerkan fasa SmA '*intercalated*'. Penyusunan '*intercalated*' ialah hasil daripada, sekurang-kurangnya sebahagiannya, interaksi lebih sesuai antara dua teras mesogenik berbeza. Dimer tidak bersimetri dalam siri kedua iaitu α -(4-benzilidinakloroanilina-4'-oksi)- ω -[(4-(tiofena-2-karboksil)benzilidinaanilina-4'-oksi]-alkana dengan spaser yang terdiri daripada C₅H₁₀ sehingga C₁₂H₂₄ adalah mesogen enantiotropik. Sifat nematogenik ini menunjukkan tentang pengaruh tarikan terminal antara teras 4-benzilidinakloroanilina dan tiofena-2-karboksilat. Kesan ganjil-genap yang kuat dari segi suhu peralihan nematik-isotropik dimer ini juga telah direkodkan. Dalam siri ketiga oligomer, trimer bersimetri 4,4'-bis{ ω -[2-metilbutil-4'-(4''-fenil)benzoatoksi]alkiloksi-benzilidina}-1,4-diaminobenzena adalah nematogen dan smektogen kiral. Selain daripada fasa nematik kiral, setiap homolog dalam siri ini juga mempamerkan fasa SmA secara enantiotropik. Fasa SmC kiral feroelektrik juga diperhatikan untuk homolog dengan spaser daripada C₅H₁₀ sehingga C₉H₁₈. Tambahannya, ahli-ahli ganjil mempamerkan fasa biru dan fasa smektik bertertib-tinggi. Dua lagi siri trimer dengan kumpulan tertutukarganti lateral iaitu 4,4'-bis{ ω -[2-metilbutil-4'-(4''-fenil)benzoatoksi]-3-metoksi-4-alkiloksibenzilidina}-1,4-

diaminobenzena dan 4,4'-bis{ ω -[2-metilbutil-4'-(4''-fenil)benzoatoksi]-3-bromo-4-alkiloksibenzilidina}-1,4-diaminobenzena telah disediakan. Dengan kehadiran kumpulan metoksi lateral, empat trimer genap mempamerkan fasa nematik kiral enantiotropik sementara ahli ganjil tidak bersifat mesogenik. Sementara itu, setiap trimer tertukarganti-Br dalam siri mempamerkan fasa nematik kiral enantiotropik kecuali trimer dengan spaser C_5H_{10} dan $C_{11}H_{22}$. Sementara trimer C_5H_{10} tidak mesogenik, ahli dengan $C_{11}H_{22}$ mempamerkan fasa nematik kiral monotropik. Trimer dengan spaser C_7H_{14} dan C_9H_{18} juga menunjukkan fasa biru. Kestabilan terma yang rendah dan sifat nematogenik trimer dengan kumpulan tertukarganti lateral adalah hasil daripada halangan lateral untuk interaksi antara-molekul. Dalam siri keenam oligomer, trimer tidak bersimetri 4-etil- dan 4-floroanilinabenzilidina-2',4'-oksibis(4''-halogenoanilinabenzilidina-4'''-oksi)alkana mengandungi sama ada atom klorin atau bromin terminal. Trimer ini juga berbeza antara satu sama lain daripada segi spaser C_4H_8 and C_6H_{12} . Trimer ini adalah nematogenik dengan suhu peralihan yang rendah disebabkan arkitektur molekul bercabang. Tiga daripada homolog dengan kumpulan etil juga merupakan nematogen kekacaan dengan suhu peralihan kaca kurang daripada 15°C .

SYNTHESIS AND MESOMORPHIC PROPERTIES OF SYMMETRIC AND NON-SYMMETRIC MULTI-FUNCTIONALIZED OLIGOMERS

ABSTRACT

Six series of novel symmetric and non-symmetric oligomers with multi-functional groups have been synthesized and characterized. The oligomers comprise two series of non-symmetric dimers, three series of symmetric trimers and one series of non-symmetric trimers. The first series of non-symmetric dimers, α -(4-benzylidene-substituted-aniline-4'-oxy)- ω -[2-methylbutyl-4'-(4''-phenyl)benzoateoxy]alkanes consists of ten homologues varying in terms of terminal substituents, X = H, CH₃, F, Cl and Br as well as C₆H₁₂ and C₈H₁₆ spacers. The dimers exhibit the enantiotropic nematic phase except compounds with X = H. Both Br-substituted dimers also exhibit the intercalated SmA phase. The intercalated arrangement is the result, at least in part, of the more favourable interaction between the two unlike cores. The non-symmetric dimers in the second series, α -(4-benzylidenechloroaniline-4'-oxy)- ω -[4-(thiophene-2-carboxyl)benzylideneaniline-4'-oxy]alkanes with spacers ranging from C₅H₁₀ to C₁₂H₂₄ are all enantiotropic mesogens. The nematogenic properties indicate the predominant terminal attraction between the 4-benzylidenechloroaniline and thiophene-2-carboxylate cores. Strong odd-even effect in terms of the nematic-isotropic transition temperatures of the dimers has also been recorded. In the third series of oligomers, the symmetric trimeric 4,4'-bis{ ω -[2-methylbutyl-4'-(4''-phenyl)benzoateoxy]alkyloxybenzylidene}-1,4-diaminobenzenes are chiral nematogens and smectogens. Apart from the chiral nematic phase, every homologue in this series also exhibits the SmA phase enantiotropically. The chiral SmC phase is also observed for the homologues with spacers from C₅H₁₀ to C₉H₁₈. Additionally, the odd members exhibit the blue phase and monotropic high-order smectic phase. Another two series of trimers with lateral substituents namely the 4,4'-bis{ ω -[2-methylbutyl-4'-(4''-phenyl)benzoateoxy]-3-methoxy-4-alkyloxybenzylidene}-

1,4-diaminobenzenes and 4,4'-bis{ ω -[2-methylbutyl-4'-(4''-phenyl)benzoateoxy]-3-bromo-4-alkyloxybenzylidene}-1,4-diaminobenzenes have been prepared. With the presence of lateral methoxy groups, the four even trimers exhibit the enantiotropic chiral nematic phase whilst the odd members are not mesogenic. On the other hand, every Br-substituted trimer in the series exhibits the enantiotropic chiral nematic phase except the trimers with C_5H_{10} and $C_{11}H_{22}$ spacers. Whilst the C_5H_{10} trimer is not mesogenic, the member with $C_{11}H_{22}$ spacers exhibits the monotropic chiral nematic phase. The trimers with C_7H_{14} and C_9H_{18} spacers also show the blue phase. The lower phase thermal stability and nematogenic behaviour of the trimers with lateral substituents is the result of lateral hindrance for intermolecular interaction. In the sixth series of oligomers, the non-symmetric trimeric 4-ethyl- and 4-fluoroanilinebenzylidene-2',4'-oxybis(4''-halogenoanilinebenzylidene-4'''-oxy)alkanes incorporate either a terminal chlorine or bromine atom. The trimers also vary from each other in terms of C_4H_8 and C_6H_{12} spacers. The trimers are nematogenic with low transition temperatures due to the branched molecular architecture. Three of the members with ethyl group are also glassy nematogens with glass transition temperatures less than 15°C.

1.0 INTRODUCTION

1.1 Liquid crystals: History

Liquid crystals are fascinating materials which have been utilized in many types of applications such as display devices. The first liquid crystal compound named cholesteryl benzoate was found in 1888 by F. Reinitzer (Kelker and Hatz, 1980). His initial observation uncovered that the compound possessed two distinctive phase transitions at 146.6 °C and 180.6 °C, respectively. The substance exhibited iridescent colours in between these transition temperatures which were characteristic of a state later known as liquid crystal. By the 20th century, the correlating principles of liquid crystals and molecular structures had been developed by D. Vorländer. In general, as cited by Kelker and Hatz, the terminology of liquid crystals accepted today is based on the original work by G. Friedel. His pioneering work via polarizing microscopic observation introduced the terms such as nematic and smectic phases which have been used widely until today.

1.2 Liquid crystals: Concept

Liquid crystal is known as the fourth state of matters besides solid, liquid and gas. As shown in figure 1.1, liquid crystal is an intermediate phase between a crystal and a liquid. It is important to mention that, in relative terms, only a small percentage of chemical compounds possess liquid crystalline properties. Most substances known today have only two phase transitions with respect to the increase of temperature. The two transitions are melting and boiling. However, a liquid crystal is different from conventional compounds as it has at least another phase transition to the liquid crystalline phase from the crystalline phase before clearing to the isotropic liquid.

For discussion on liquid crystals, the liquid-gas transition is not of interest because in the gas phase, molecules are in total random motion and do not possess any degree of ordering. The difference between these two phases is the molecules of a gas is widely separated from one another and move in a path largely unaffected by intermolecular forces.

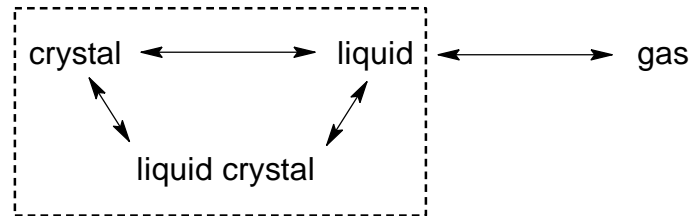


Figure 1.1: Primary phase transitions and phase transitions involving liquid crystalline phase (in dotted box)

1.3 Mesophases

The liquid crystalline phase is known as mesophase. There are many mesophases which have been discovered but these phases can be categorized into two major ones; nematic and smectic phases. The nematic phase is exhibited at higher temperature in comparison to the smectic phase. The nematic phase has more similarities to the liquid phase whilst the smectic and crystal phase are more similar to each other.

1.3.1 Nematic phase

In the nematic phase, the molecules possess some degree of orientational order. In average, the molecules are all aligned towards similar direction in the nematic phase. The orientational direction is represented by the director (figure 1.2). There is no positional ordering in the nematic phase.



Figure 1.2: Nematic phase (Barón, 2001)

1.3.1.1 Chiral nematic phase

The chiral nematic phase is also known as the cholesteric phase. In the chiral nematic phase, the chiral center of every molecule provides intermolecular force which enables molecules to align at a slight angle from one another. This leads to a stack of nematic layers with the local director in each layer twisted around a single axis as illustrated in figure 1.3. The overall molecular orientation in the chiral nematic phase is visualized as a continuous twisting pattern like a helix from one layer to another.

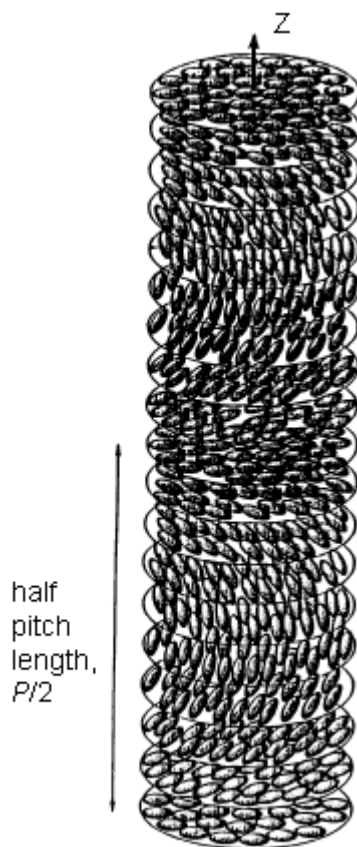


Figure 1.3: Chiral nematic phase (Barón, 2001)

1.3.2 Smectic phase

Unlike the nematic phase, the smectic phase possesses some similarities to the crystal phase as the smectic molecules are arranged in layer-like ordering. In other words, there exist positional orders in a smectic phase. In the smectic phase, the molecules also possess orientational order which is similar to that of a nematic phase.

1.3.2.1 Non-chiral smectic phase

Based on the differences in molecular orientation and packing in the smectic layers, more than ten different smectic modifications have been reported. The simplest smectic phase is known as the smectic A (SmA) phase. In the SmA phase, molecules are aligned perpendicular to the smectic plane as shown in figure 1.4(a). In the layers, molecules do not have any particular positional order. The SmA phase has been observed in various liquid

crystalline compounds such as the 5,5'-substituted-2,2'-bipyridines with flexible alkoxy terminals (Douce *et al.*, 1996).

The SmA phase can be further classified into different types such as the monolayer, bilayer, interdigitated and intercalated SmA phase. The monolayer SmA phase (SmA₁) is the simplest SmA phase and is the most frequently encountered SmA phase. The SmA₁ layer thickness corresponds to the length of the molecule. Bilayer SmA (SmA₂) phase with layer spacing twice the molecular length is usually observed for liquid crystals with a terminal dipolar group such as cyano or nitro group. This is due to the electrostatic interaction arising from the opposite direction of longitudinal component with regard to the cyano or nitro dipoles (Madhusudana, 2001). In the interdigitated SmA (SmA_d) phase, the layer thickness is more than the length of one molecule but less than the length of two molecules. The SmA_d phase is usually observed for liquid crystals with two different mesogenic cores in the molecular structure. The driving force for this phase is however not confined to only the presence of two unlike cores in the structure, as electrostatic interaction between certain groups like the polar and polarizable cyanobiphenyl groups is known to play a key role in inducing interdigitation. The length of the terminal flexible chain is also important in the sense that if the chain length is more than the length of the flexible core, the long terminal chain cannot be accommodated in the available space leading to the formation of interdigitation (Attard *et al.*, 1994). Contrary to SmA_d, the smectic layer periodicity in the intercalated SmA (SmA_c) phase is approximately half the molecular length. The intercalation, which often occurs among the non-symmetric dimers, results from a specific interaction between the unlike mesogenic cores enhanced by an entropy gain resulting from the uniform mixing of such groups (Blatch *et al.*, 1997). The observations of SmA_c phase for symmetric dimers is less common, but nevertheless, it has also been reported for the symmetric dimers incorporating two biphenyl groups with terminal OC₄H₉ groups. The intercalated smectic phase is possibly driven by an interaction between the carbonyl groups

which link the spacer to the mesogenic units and the ether groups which connect the terminal chains to the mesogenic moieties (Attard *et al.*, 1994 and Watanabe *et al.*, 1993).

The smectic C (SmC) phase is the tilted analogue of the SmA phase. In each SmC layer, molecules are arranged in similar order as in SmA phase. However, as illustrated in figure 1.4(b), in every SmC layer, molecules are tilted at a constant tilt angle (θ) with respect to the layer normal. From X-ray diffraction analyses, reports have shown that for a number of liquid crystal materials, the θ in the SmC phase is temperature dependent. In other words, the θ of the SmC molecules may increase or decrease with respect to the changing of temperature.

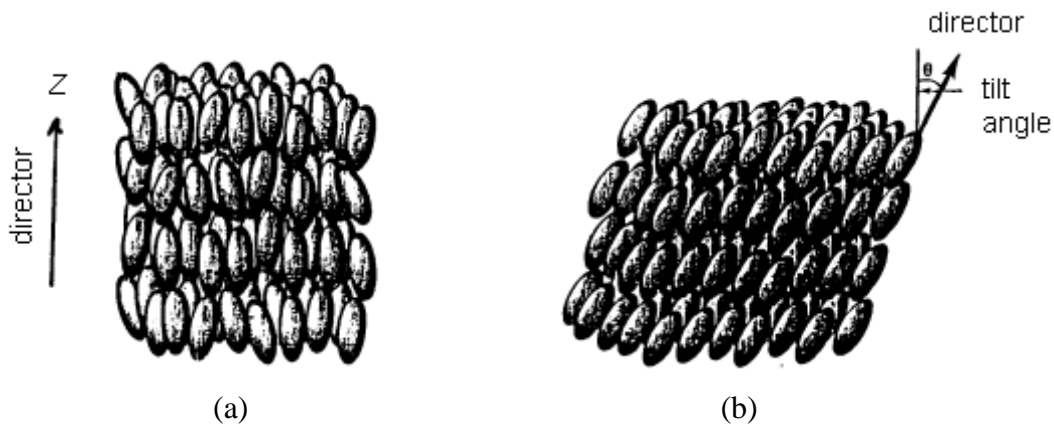


Figure 1.4: Molecular arrangement in (a) SmA phase with $Z =$ optic axis;
(b) SmC phase (Barón, 2001)

Apart from the SmA and the SmC phases of which the layers are unstructured, the hexatic smectic phases namely the SmB, SmF and SmI phases have also been observed. In the SmB phase, the director is perpendicular to the layers with long-range hexagonal bond-orientational order. The bond-orientational order represents the long range orientational but short range positional ordering of molecules within a smectic layer (Dierking, 2003). The illustration of the molecular organization in a SmB phase is given in figure 1.5.

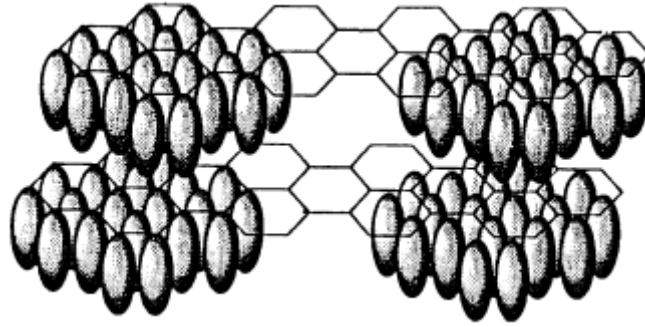


Figure 1.5: SmB phase (Barón, 2001)

Contrary to the SmB phase, the director in the SmF and SmI phases is tilted with respect to the layer normals. For the SmF phase, the director is tilted towards the side of the hexagons as shown in figure 1.6(a). On the other hand, the molecules in the SmI phase tilt towards the apex of the hexagon (figure 1.6(b)). The in-plane positional correlations in the SmI phase are slightly greater than in the SmF phase.

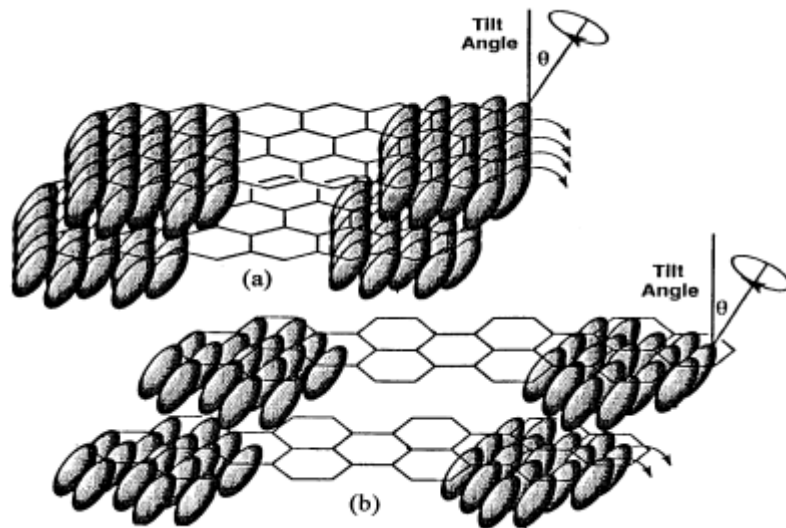


Figure 1.6: Illustration of the respective tilt directions of the director in the (a) SmF; (b) SmI phases

1.3.2.2 Chiral smectic phase

The chiral smectic C (SmC^*) phase is one of the most widely discussed chiral smectic phases (Lunkwitz *et al.*, 1998 and Hamaneh and Taylor, 2005). A host of materials exhibiting the SmC^* phase have been synthesized such as the mesogenic derivatives of 2S,3S-2-halogeno-3-methylpentanoic acid (Szydłowska *et al.*, 1999). In the similar manner to SmC phase, in every layer molecules are tilted at a constant tilt angle with respect to the axis perpendicular to the plane. In addition to this, the SmC^* molecules are arranged in a macroscopic helical pattern as the result of precession of the tilt about the same axis from one layer to another (figure 1.7). For a particular material, the rotation always occurs in the same direction whether it is left-handed or right-handed (Singh, 2002).

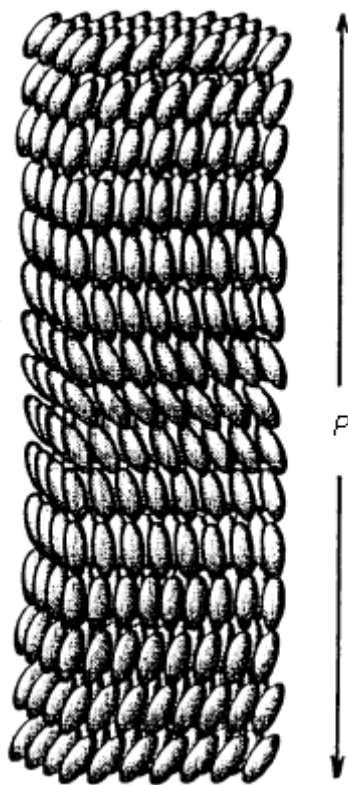


Figure 1.7: SmC^* phase with P = helical pitch (Barón, 2001)

1.3.2.3 Unidentified smectic phase

Irrespective of whether the liquid crystals are optically active or not, there have been few cases whereby a smectic phase cannot be determined conclusively by powder X-ray diffraction, mesophase texture observation and even miscibility studies. In such cases, the smectic phase is often called as smectic X (SmX) which represents an unidentified smectic phase. One such example is exhibited by the five-ring λ -shaped mesogenic compounds of which three unidentified smectic phases have been observed (Yamaguchi *et al.*, 2005). Another example of unidentified smectic phase has also been discussed for a laterally fluorinated banana-shaped liquid crystal (Lee *et al.*, 2001).

1.3.3 Blue phase

The blue phase is often observed in between the chiral nematic phase and the isotropic phase. In terms of structure, the blue phase possesses three-dimensional spatial distribution of helical director axes leading to a frustrated structure as shown in figure 1.8 (Meiboom *et al.*, 1981 and Barón, 2001). Within every double twist cylinder, the local director rotates around any given radius of the cylinder. At the core of the cylinder, the director is oriented parallel to the cylinder long axis. On moving outwards, the local director twists along any radius until the twist angle is approximately 45° at the edge of the double twist cylinder. The blue phase only exists in chiral liquid crystalline materials with smaller helical pitch (Stegemeyer, 1999). This characteristic has been reported for the non-symmetric dimers with odd parity of which the pitch is smaller in comparison to the even counterparts (Blatch *et al.*, 1997). Other examples of liquid crystals which have also exhibited the blue phase are the three-ring terephthalates with four ester linkages (Fodor-Csorba *et al.*, 1998).

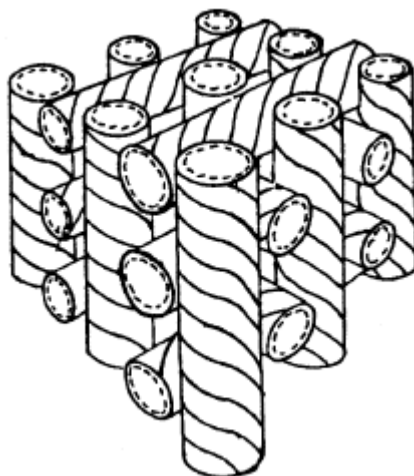


Figure 1.8: A blue phase model consisting of double-twist cylinders forming a cubic lattice (Barón, 2001)

1.4 Mesogen

A mesogen is a compound which can exist as a liquid crystal phase under suitable conditions of pressure, temperature and concentration. Based on the aspect of molecular structure, mesogens can be divided to several types including the calamitic, discotic, banana-shaped, laterally branched and oligomeric systems.

1.4.1 Calamitic mesogens

Calamitic mesogens are also known as rod-like mesogens due to the linearity of the molecular structure. As such, majority of calamitic mesogens involves *para-para* aromatic substitutions to give the rod-like structures. Calamitic mesogens possess high shape anisotropy which are favourable for layered molecular arrangement in the mesophase. Two examples of calamitic mesogens are shown in figure 1.9(a) and (b).

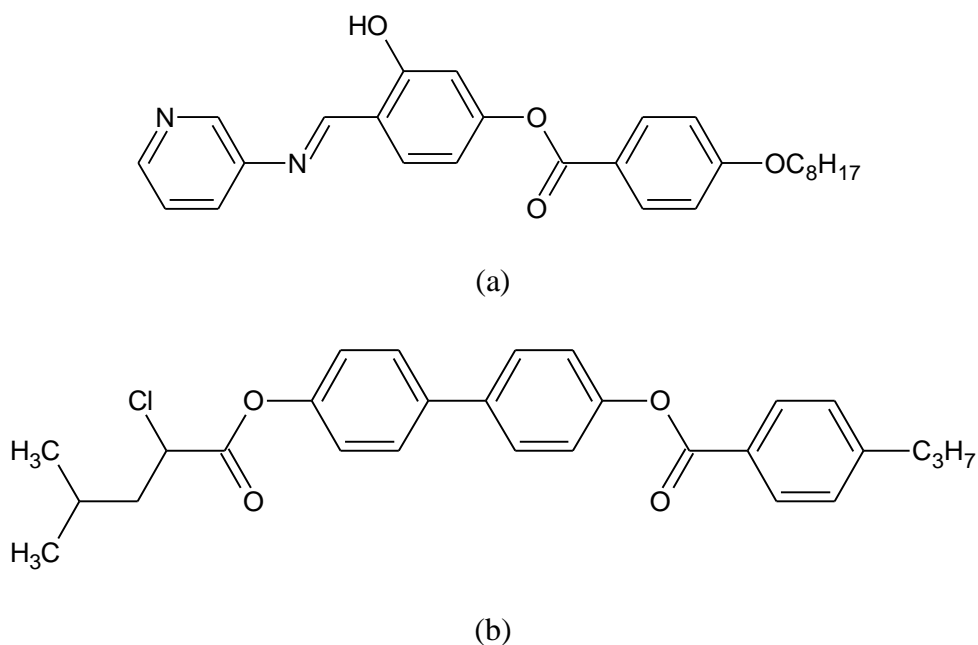


Figure 1.9: Two examples of calamitic mesogens (a) N-[4-(4-octyloxybenzoyloxy)-2-hydroxybenzylidene]-3-aminopyridine (Takase *et al.*, 2003); (b) 4-[(S)-2-chloro-4-methylpentanoyloxy]-4'-[4-propylbenzoyloxy]biphenyl (Schacht *et al.*, 1998)

1.4.2 Discotic mesogens

Discotic mesogens are mesogens with disc- or sheet-shaped structures. The mesophases formed by columnar stacking of discotic mesogens are called the columnar mesophases. An example of discotic mesogen is shown in figure 1.10.

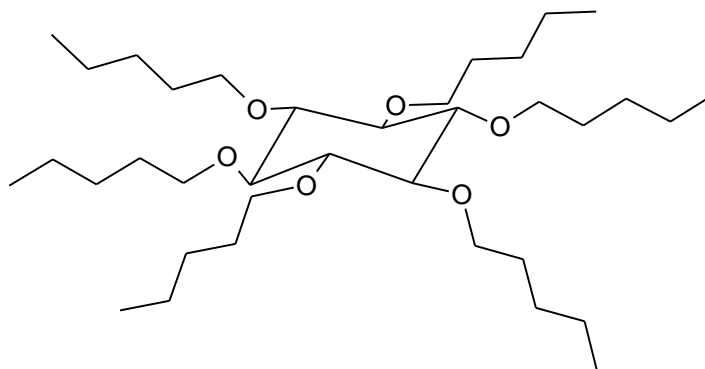


Figure 1.10: Inositol ether (Tschierske, 1998)

1.4.3 Banana-shaped mesogens

Banana-shaped mesogens possess the bent molecular structure due to the 1,3-aromatic substitution at the center of the rigid mesogenic core. Due to the unique bent structure, banana-shaped liquid crystals exhibit unconventional mesophases such as the B₆ mesophase and few chiral mesophases even if the molecules do not contain any chiral centers. An example of banana-shaped liquid crystals is 4,6-dichloro-1,3-phenylenebis[4-(4-*n*-octyloxyphenyliminomethyl)benzoate] with the molecular structure as shown in figure 1.11 (Lee *et al.*, 2003).

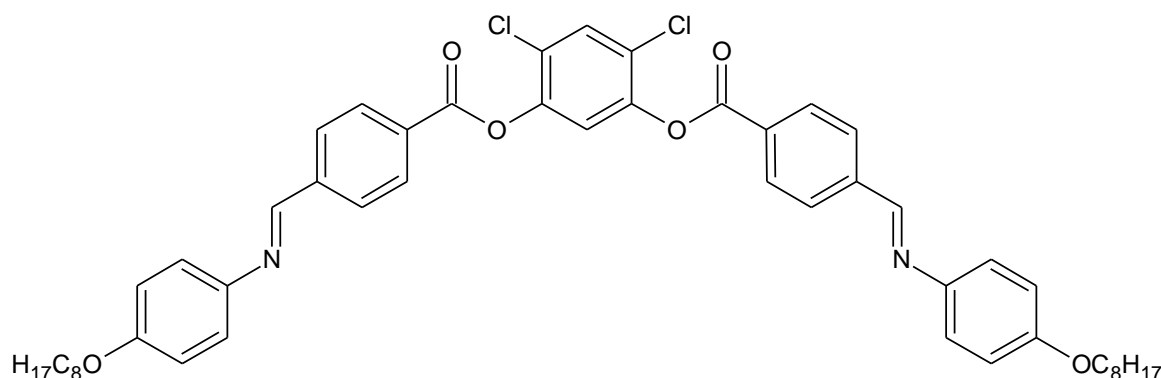


Figure 1.11: 4,6-Dichloro-1,3-phenylenebis[4-(4-*n*-octyloxyphenyliminomethyl)-benzoate] (Lee *et al.*, 2003)

1.4.4 Laterally branched mesogens

An alkyl or aromatic group can be introduced to a calamitic mesogen at a lateral position to form the laterally branched mesogen. Until 1983, it was generally accepted that a lateral substituent would diminish the liquid crystalline properties with the extent of the effect depending on the size of substituent. However, in 1983 and 1984, it was then found that compounds with large flexible lateral substituents are also mesogenic as well (Vora and Prajapati, 2002). Since then, a host of novel compounds with different type of lateral substituents have been reported. The molecular structure for one of these compounds is shown in figure 1.12. However, vast majority of these reported laterally branched mesogens

are monomeric, e.g. not oligomeric, in terms of molecular constitution. As such, the mesogenic group is present as one interconnected unit as a whole with the flexible alkyl groups either attached at the terminals or as lateral substituent itself.

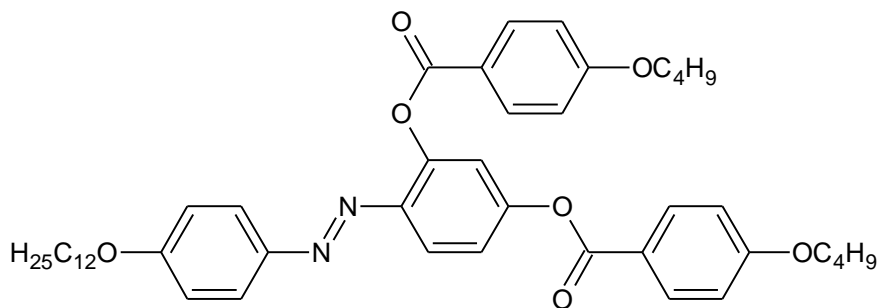
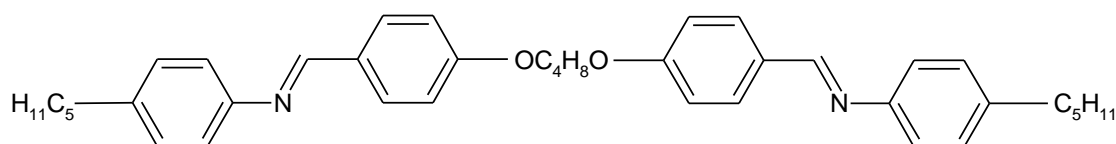


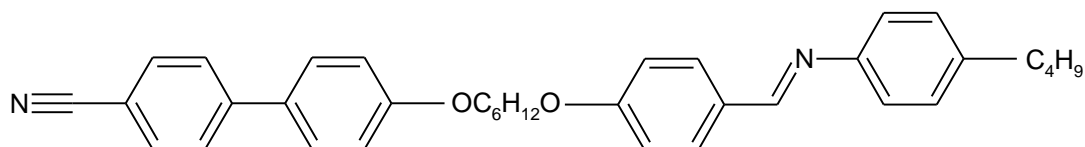
Figure 1.12: 4-Dodecyloxy-2'-(4-butoxybenzoyloxy)-4'-(4-butoxybenzoyloxy)-azobenzenes (Berdagué *et al.*, 1993)

1.4.5 Oligomeric mesogens

Oligomeric mesogens have been given considerable amount of attention as these compounds are used as models for the semi-flexible main chain liquid crystal polymers (Imrie and Henderson, 2002 and Pal *et al.*, 2007). The shortest liquid crystal oligomer, the dimer consists of two mesogenic units connected by one flexible group called the spacer in every molecule. A symmetric dimer possesses two identical mesogenic fragments. However, the mesogenic units may not be necessarily the same to each other. In the case where the mesogenic units are different from each other, non-symmetric liquid crystal dimers are formed. The examples of symmetric and non-symmetric dimers are shown in figure 1.13(a) and (b), respectively.



(a)



(b)

Figure 1.13: Respective example of symmetric dimer and non-symmetric dimer
 (a) α,ω -bis(4-pentylanilinebenzylidene-4'-oxy)butane (Date *et al.*, 1992);
 (b) α -(4-cyanobiphenyl-4'-oxy)- ω -(4-butylanilinebenzylidene-4'-oxy)-hexane (Hogan *et al.*, 1988)

Recently, another series of non-symmetric dimers have been reported, of which the dimers contain cholesterol and 4-(*trans*-4-*n*-hexylcyclohexyl)benzoic acid moieties linked with the central spacer through two ester bonds (Yu *et al.*, 2008). The general structure of the dimer is given in figure 1.14.

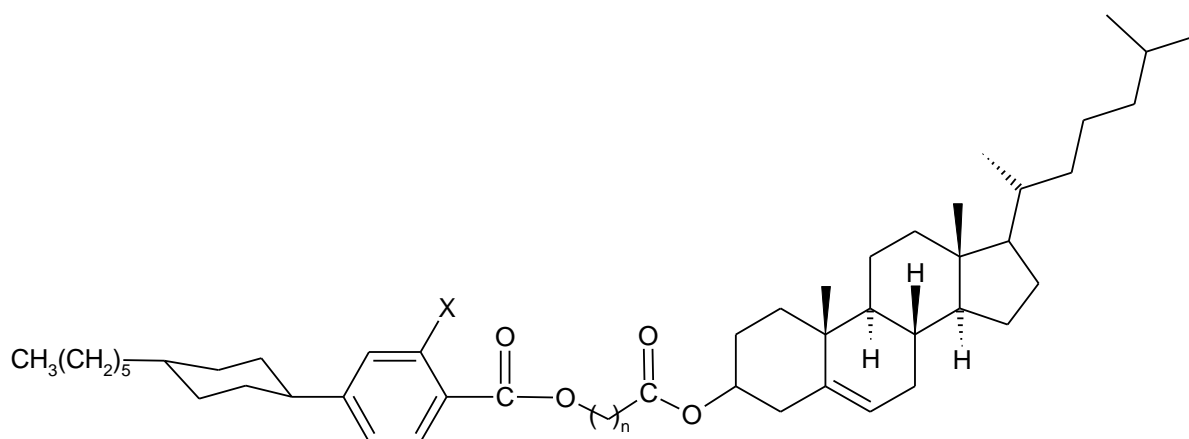


Figure 1.14: Structure for the dimer which contains cholesterol and 4-(*trans*-4-*n*-hexylcyclohexyl)benzoic acid moieties (Yu *et al.*, 2008)

The trimeric liquid crystals contain three mesogenic cores separated by two flexible spacers in every molecule. In a similar manner to liquid crystal dimers, the trimers can be

non-symmetric as well. For trimers, the asymmetry can be introduced to the structure by incorporating two spacers with different number of methylene units or two different mesogenic cores. A trimer can also be non-symmetric by having an asymmetric central core despite having both terminals identical to each other. The examples of symmetric and non-symmetric trimers are depicted in figure 1.15(a) and (b), respectively.

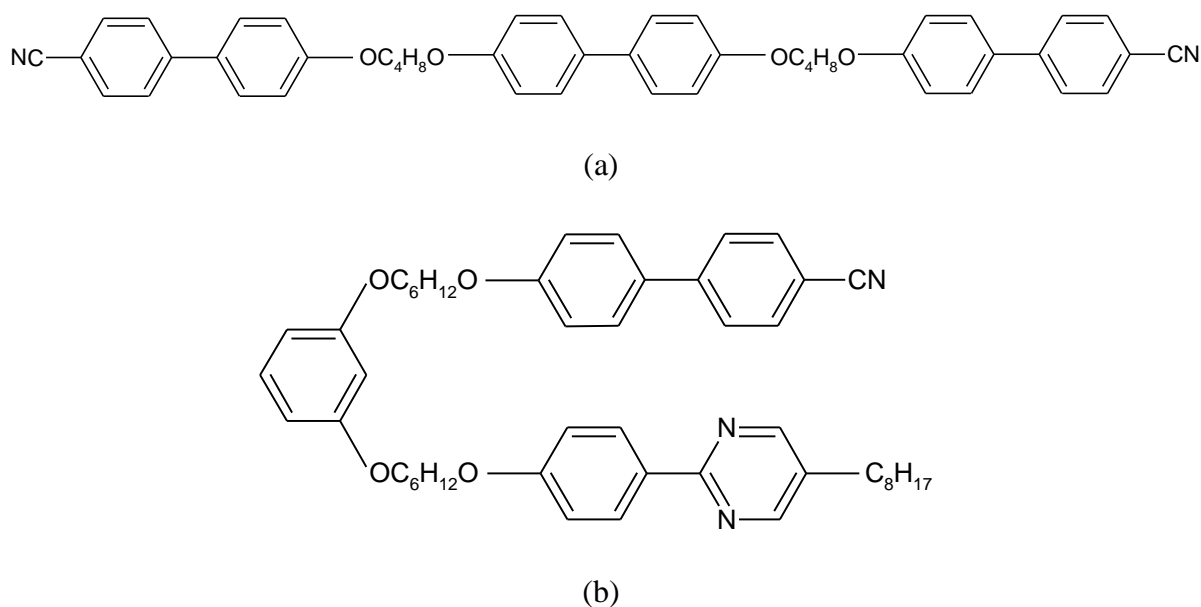


Figure 1.15: Respective example of symmetric trimer and non-symmetric trimer
 (a) 4,4'-bis[ω -(4-cyanobiphenyl-4'-yloxy)butyloxy]biphenyl;
 (b) mesogen incorporating 5-octylpyrimidine-2-yl and 4-cyanophenyl moieties (Yoshizawa *et al.*, 2005)

1.5 Structure-property relationship of liquid crystals

The liquid crystalline properties of mesogenic compounds are governed by the molecular structures and the attributes as the result of these structures. It is known that by substituting certain atom or group of atoms in a molecule, the liquid crystalline properties may also be altered. The correlation between chemical constitution and liquid crystalline properties of which is available today is largely based on the early work by D. Vorländer, C. Weygand, C. Wiegand and G. W. Gray (Kelker and Hatz, 1980). The general criteria in order for molecules to be mesogenic are as follow:

- a) The most favourable geometry of liquid crystal molecules is rod-like and narrow reflecting high shape anisotropy.
- b) The molecules possess high anisotropy of polarizability.
- c) The melting point of the compound must not be too high.
- d) Permanent dipolar groups are present in the molecules.

1.5.1 Structure-property relationship of liquid crystal oligomers

1.5.1.1 The influence of spacer length and parity on the liquid crystalline properties of oligomers

Previous researches have shown that the liquid crystalline properties of oligomeric mesogens are strongly dependent on the length and parity of the flexible spacers, in a manner strongly reminiscent of that seen for the semi-flexible main chain liquid crystalline polymers (Henderson and Imrie, 2005). In a homologous series for instance, the dimers and trimers with shorter spacers may exhibit liquid crystalline properties which differs from those observed for the longer counterparts. One of such unique characteristics which have been noted for the symmetric dimers is the decreasing tendency to exhibit smectogenic properties upon increasing spacer length (Date *et al.*, 1992).

In general, the dependence of transition temperatures of oligomers upon substituting the spacers with different number of methylene units, n can be observed as the zigzag alternation pattern of which the temperature is often lower for the homologues with odd-parity spacers. For example, in a series of eight-ring tetramers with two azo and two Schiff base linkages, the melting points exhibited pronounced alternation as n was increased although attenuation was not observed upon ascending this series (Henderson and Imrie, 2005). The behaviour is explained by the change in conformational statistical weights of the spacer on melting into a nematic phase is small for an even-parity spacer but large for an odd-parity spacer. This behaviour may also reflects that the tetramers with even spacers

which presumably adopt more elongated conformations, pack more efficiently into a crystal lattice than the odd counterparts, which adopt, on average, bent molecular shapes.

1.5.1.2 The influence of unlike cores and non-symmetric structures on the liquid crystalline properties of oligomers

The non-symmetric oligomers exhibit liquid crystalline properties differently from the oligomers with symmetric molecular architectures. In recent years, the non-symmetric oligomers have been increasingly given attention by researchers to understand how these non-symmetric molecules interact with each other especially to exhibit smectic phases with untypical layer periodicities. One of such examples is the α -(4-cyanobiphenyl-4'-yloxy)- ω -[4-(5-alkylpyrimidine-2-yl)phenyl-4''-oxy]alkanes of which the observed smectic phases are either intercalated or interdigitated in nature (Yoshizawa *et al.*, 2006). The details on the intercalated and interdigitated smectic phases have been described in section 1.3.2.1.

1.5.2 Chirality effect on liquid crystalline properties

Chirality is an inherent property of many natural systems such as DNA and enzymes. In liquid crystals, chirality can be introduced in several different ways. It can be introduced within the mesogen by incorporation of chiral centers. Another way which is more commonly practiced in producing materials for applications is the addition of chiral dopant to an achiral host phase (Dierking, 2003).

The presence of one or several chiral centers in a mesogen can tremendously modify the organization of the mesophases (Pansu, 2003). For instance, novel structures like the helical superstructures of the N* and SmC* phases can be induced. The physical properties of mesophases are modified by the loss of mirror symmetry. Tilted chiral smectic phases can exhibit spontaneous polarization and thus these mesophases are pyroelectric (Dierking, 2003).

1.6 Application of liquid crystals

Liquid crystals have been widely used in many high-tech applications such as displays. Liquid crystal displays have dominated the flat panel technology in products such as LCD television and personal digital assistant (PDA). A flat display typically contains a thin layer of liquid crystalline mixture in between two extremely thin glass plates with transparent electrodes twisted by 90° from each other. Polarizing filters are positioned at the outside of the plates whilst the colour filter, transparent electrodes and orientation layers are situated at the inside. The first polarizing filter only allows light of only a particular plane of oscillation to pass through it and subsequently reaches the liquid crystals. The applied voltage orients the molecules perpendicular to the glass plates. The light follows this new orientation and is unable to pass through the second filter which is at 90° to the first filter. Therefore the pixel is black. By removing the voltage, the molecules return to the original twisted arrangement. The light follows this twist and is now able to traverse the second filter to give a bright pixel. A liquid crystal display contains millions of pixels. The bright and dark pixels produce a pattern which gives the desired image.

Apart from liquid crystal displays, the natural characteristics of liquid crystalline phases have also been exploited for the development of other technological applications. For instance, the helical structures in the chiral smectic C and chiral nematic phases have been recognized for their use in electro-optic and thermochromic devices, respectively (Hemine *et al.*, 2007 and Yelamaggad and Shanker, 2008). Besides, the electroclinic property of the orthogonal layered phase, the chiral smectic A phase holds great promise in spatial light modulation applications (Yelamaggad and Shanker, 2008).

Whilst the monomeric form of liquid crystals have been widely used in various technological devices, the application of the liquid crystalline oligomers mainly lies in serving as a research model for the industrially important semi-flexible main chain liquid crystalline polymers. This is possible due to the similarities in terms of liquid crystalline

transitional properties between the oligomers and polymeric systems based on previous findings (Attard *et al.*, 1994 and Imrie and Luckhurst, 1998). In the industries, the liquid crystalline polymers are utilized in the production of high strength fibers. Compared to other polymers, liquid crystalline polymers are advantageous as these materials possess outstanding properties such as high resistance to extreme weathers, radiation, burning and almost all chemicals. Such characteristics of liquid crystalline polymers make them highly suitable to replace other conventionally used materials including metals. The type of liquid crystalline polymers produced is dependent on the incorporated functional groups, for example, terephthalic acid and 4-hydroxybenzoic acid. The concept in the making of these high-strength materials firstly involves the orientation of the polymers in the desired liquid crystalline phase and subsequently quenching to produce highly ordered solid.

1.7 Objectives of the research

The unique relationship between chemical constitution of liquid crystals and the induced mesomorphic characteristics has made the syntheses of novel mesogens an exciting area of research. Over the years, through rigorous investigations, many significant and interesting findings have been reported including:

- a) Intercalated and interdigitated smectic phases
- b) Reentrant mesophases (Pal *et al.*, 2007)
- c) Host of chiral mesophases including the ferroelectric SmC* phase (Liao *et al.*, 2006)
- d) Mesogens with unconventional shapes such as H and λ shapes

These findings have deepened our understanding on liquid crystals as well as triggered the keenness in many researchers, including myself, to explore further. In addition to the numerous interesting findings on liquid crystals in general, the unconventional liquid

crystalline properties of oligomers have also been inspirational leading to our preparation of six series of novel dimers and trimers incorporating various mesogenic groups. In the Liquid Crystal Research Laboratory, my PhD research project was conducted based on these six objectives:

- a) To synthesize a host of new liquid crystal dimers and trimers which are symmetric and non-symmetric in terms of molecular architecture
- b) To study the molecular organization of the dimeric and trimeric molecules in the nematic and smectic phase and how structural asymmetry may influence the molecular arrangement and induce unconventional mesophases
- c) To investigate the impact of chirality on liquid crystalline properties of trimers
- d) To uncover how different substituents at certain positions in the mesogenic fragment can influence the liquid crystalline properties as well as mesophase thermal stability
- e) To make comparison and extend our research findings on the novel dimers and trimers in terms of spacer dependent odd-even effect to the polymeric system
- f) To study the impact of lateral branching on the trimers in terms of presence or absence of certain mesophases and suppression in transition temperatures

2.0 EXPERIMENTAL

2.1 Chemicals

The fine chemicals used for the syntheses of compounds were purchased from major companies including Merck, Acros Organics, Sigma-Aldrich, Fluka and Fisher Scientific. In addition, the purchase of several fine chemicals from Tokyo Chemical Industry was supported by Soka University, Japan. The chemicals were used directly from the bottles without further purification. The complete list of these chemicals is given in table 2.1.

Table 2.1: List of chemicals used for the syntheses and respective assays

Compound	Assay, %	Company	Assay, %
1,8-Dibromooctane ^a	≥97	1,5-Dibromopentane ^b	97
Aniline ^a	≥99	1,6-Dibromohexane ^b	98
4-Chloroaniline ^a	≥99	1,9-Dibromononane ^b	97
4-Bromoaniline ^a	≥98	1,10-Dibromodecane ^b	97
4-Methylaniline ^a	≥99	1,11-Dibromoundecane ^b	≥98
4-Ethylaniline ^a	≥98	1,12-Dibromododecane ^b	96
1,4-Diaminobenzene ^b	≥99	1,7-Dibromoheptane ^c	97
4-Aminophenol ^b	98	Vanillin ^d	≥98
4-Fluoroaniline ^b	98	Potassium carbonate anhydrous ^e	≥99
4-Hydroxybenzaldehyde ^b	99	Potassium iodide ^e	≥99
2,4-Dihydroxybenzaldehyde ^b	98	4-(4-Hydroxyphenyl)benzoic acid ^f	≥98
2-Thiophenecarbonyl chloride ^b	98	(<i>RS</i>)-2-Methyl-1-butanol ^f	≥97
1,4- Dibromobutane ^b	99	(<i>S</i>)-(-)-2-Methyl-1-butanol ^f	≥98

^{a-f} chemicals obtained from Merck, Acros Organics, Sigma-Aldrich, Fluka, Fisher Scientific and Tokyo Chemical Industry in similar order

2.2 Equipment

Various chemical and physical analyses were conducted to characterize the intermediary and title compounds using instruments which are listed as follow:

1. The melting points of the compounds were determined using Gallenkamp melting point apparatus.
2. The CHN microanalyses were carried out on a Perkin Elmer 2400 LS Series CHNS/O analyzer. The samples were sealed in tin capsules prior to the analyses.
3. The Fourier Transform infrared spectroscopy (FT-IR) analyses were performed on a Perkin Elmer 2000-FTIR spectrometer. The powder samples were mixed homogenously with potassium bromide and subsequently compressed into pellets. The samples were then analyzed in the range of $4000\text{-}400\text{ cm}^{-1}$.
4. The Fourier Transform nuclear magnetic resonance spectroscopy (FT-NMR) analyses were conducted using the Bruker 300 MHz and 400 MHz UltrashieldTM spectrometers. The samples were dissolved in deuterated chloroform containing tetramethylsilane as the internal standard. Due to the partial solubility of several compounds in CDCl_3 at room temperature, the spectrometer internal heater was also used to maintain the NMR sample temperature at $55\text{ }^{\circ}\text{C}$ from the point at which the shimming and wobbling was initiated until the scans were completed.
5. The liquid crystalline texture for the compounds were observed using a Carl Zeiss Axioskop 40 polarizing optical microscope equipped with a Linkam TMS94 temperature controller, LTS350 hot-stage and LNP cooling system. For additional optical texture studies, the homeotropic alignment was achieved by coating the microscope slides and glass covers with stearic acid dissolved in chloroform prior to deposition on the surface. The evaporation of chloroform resulted in a thin, transparent film of the stearic acid on the glass surfaces (Dierking, 2003).

6. The thermal properties of the liquid crystals were investigated via differential scanning calorimetry (DSC) and the analyses were carried out using two different instruments as follow:

- i. Seiko DSC120 Model 5500 differential scanning calorimeter at Faculty of Engineering, Soka University, Tokyo, Japan
- ii. Seiko DSC6200R differential scanning calorimeter at Chemical Resources Laboratory, Tokyo Institute of Technology, Yokohama, Japan

The heating and cooling rates of the Seiko DSC120 Model 5500 and DSC6200R differential scanning calorimeters are $\pm 2\text{ }^{\circ}\text{Cmin}^{-1}$ and $\pm 5\text{ }^{\circ}\text{Cmin}^{-1}$, respectively. For every series of compounds, only one model of differential scanning calorimeter was used to ensure that the thermal properties of the compounds in that series are comparable to one another.

7. The powder X-ray diffraction analyses were performed on a Bruker D8 diffractometer equipped with a Göbel mirror, Vantec linear detector and vertical goniometer at Department of Chemistry, Warsaw University, Warsaw, Poland. Sample temperature was controlled by Anton Paar heating stage and the θ - θ scans were performed every $0.5\text{ }^{\circ}\text{C}$.

2.3 Synthesis and characterization

All compounds were synthesized, recrystallized and analyzed at standard atmospheric pressure of 101.325 kPa.

2.3.1 First series

α -(4-Benzylidene-substituted-aniline-4'-oxy)- ω -[2-methylbutyl-4'-(4''-phenyl)-benzoateoxy]alkanes, **4a-4j**

The overall synthetic routes towards obtaining α -(4-benzylidene-substituted-aniline-4'-oxy)- ω -[2-methylbutyl-4'-(4''-phenyl)benzoateoxy]alkanes, **4a-4j** are shown in figure 2.1. The experimental procedure for every step is given from section 2.3.1.1 to 2.3.1.4.

2.3.1.1 Synthesis of (*RS*)-2-methylbutyl-4'-(4''-hydroxyphenyl)benzoate, **1**

4-(4-Hydroxyphenyl)benzoic acid (1.50 g, 7.0 mmole) was dissolved in 40 mL of (*RS*)-2-methyl-1-butanol in a round-bottom flask. As heat was gradually applied, catalytic amount of concentrated sulphuric acid was added slowly to the stirring mixture and refluxed at 90 °C for 24 h. After reflux, the excess (*RS*)-2-methyl-1-butanol was left at room temperature to evaporate off. The yellow precipitate was recrystallized thrice from the mixture of chloroform and hexane to give the desired white ester.

2.3.1.2 Synthesis of 4-hydroxy-4'-benzylidene-substituted-anilines, **2a-2e**

4-Hydroxybenzaldehyde (0.98 g, 8.0 mmole) was dissolved in 40 mL of absolute ethanol in a round-bottom flask. An ethanolic solution of the corresponding aniline (8.0 mmole) was then added dropwise and the mixture was refluxed for 10 h. The resulting solution was left to evaporate off at room temperature. The brown precipitate was subsequently recrystallized from chloroform to yield the desired intermediate categorized as Schiff base. The general molecular formula and amounts of corresponding anilines for the five syntheses are listed accordingly in table 2.2.